land

MDPI

Review

Assessment and Mapping of Soil Salinity Using the EM38 and EM38MK2 Sensors: A Focus on the Modeling Approaches

Panagiota Antonia Petsetidi and George Kargas *

Laboratory of Agricultural Hydraulics, Department of Natural Resources Development and Agricultural Engineering, Agricultural University of Athens, Iera Odos 75, GR11855 Athens, Greece; tpetsetidi@aua.gr
* Correspondence: kargas@aua.gr

Abstract: Soil salinization and its detrimental agricultural, environmental, and socioeconomic impact over extended regions represent a major global concern that needs to be addressed. The sustainability of agricultural lands and the development of proper mitigation strategies require effective monitoring and mapping of the saline areas of the world. Therefore, robust modeling techniques and efficient sensors that assess and monitor the spatial and temporal variations in soil salinity within an area, promptly and accurately, are essential. The aim of this paper is to provide a comprehensive and up-to-date review of the modeling approaches for the assessment and mapping of saline soils using data collected by the EM38 and EM38MK2 (MK2) sensors at different scales. By examining the current and latest approaches and highlighting the most noteworthy considerations related to their accuracy and reliability, the intention of this review is to elucidate and underline the role of the EM38 and the MK2 type in the recent needs of detecting and interpreting soil salinity. Another aim is to assist researchers and users in selecting the optimal approach for future surveys and making well-informed decisions for the implementation of precise management practices. The study's findings revealed that the integration of the EM38 and MK2 sensors with remote sensing data and advanced methods like machine learning and inversion is a promising approach to the accurate prediction and mapping of the spatiotemporal variations in soil salinity. Therefore, future research focused on validating and expanding such sophisticated modeling applications to regional and global scales should be increased.

Keywords: soil salinity; assessment; EM38; EM38MK2; ECe; models; remote sensing; monitoring; mapping

check for updates

Citation: Petsetidi, P.A.; Kargas, G. Assessment and Mapping of Soil Salinity Using the EM38 and EM38MK2 Sensors: A Focus on the Modeling Approaches. *Land* **2023**, *12*, 1932. https://doi.org/10.3390/land12101932

Academic Editors: Tiago Brito Ramos, Maria da Conceição Gonçalves and Mohammad Farzamian

Received: 19 September 2023
Revised: 10 October 2023
Accepted: 11 October 2023
Published: 17 October 2023

Copyright: © 2023 by the authors. Licensee MDPI, Basel, Switzerland. This article is an open access article distributed under the terms and conditions of the Creative Commons Attribution (CC BY) license (https://creativecommons.org/licenses/by/4.0/).

1. Introduction

Soil salinization has been considered one of the most challenging global threats, affecting large cultivated and irrigated areas all over the world. Its detrimental impacts on environmental quality, agricultural productivity, and socioeconomic stability are about to become even more pronounced in the coming years due to climate change [1]. The extent of soil salinity along with the frequency of floods and duration of droughts, as a consequence of climate change, are expected to be more intense and exacerbated in the arid and semi-arid regions where the sustainability of natural resources is imperative [2]. Considering the increasing demands for global food supplies and arable land, these effects necessitate urgent control and mitigation. For this purpose, regular and accurate monitoring of soil salinity distribution and its spatial variations across multiple scales is crucial for preventing soil salinization hazards and preserving the long-term sustainability of agricultural and environmental systems.

Successful monitoring of soil salinization requires rigorous modeling techniques and advanced tools to reliably assess the soil salinity levels and interpret its severity in different areas of the world. Recently, satellite remote sensing technology has been widely applied as an effective tool for identifying and mapping the soil salinity of large-scale areas [3].

However, the sensors are incapable of detecting the subsurface distribution of the soluble salts and the highly spatial heterogeneities in the soil profile [4]. Thus, their implementation is usually combined with other sensors or data for more accurate results [5].

On the other hand, proximal sensing (PSS) technology with ground-based, electromagnetic induction (EMI) sensors can quantify and characterize the spatial patterns of soil salinity within the soil profile by measuring the soil's apparent electrical conductivity (ECa). Besides the popular EM38 sensor, a variety of commercial EMI devices have also been developed, enabling the investigation of the solute's variability at different soil layers and allowing soil salinity mapping, particularly on the field scale [6].

Despite the accessibility of improved proximal sensing devices such as the EM38MK2 (MK2), an upgraded type of EM38, and the range of studies that evaluate various EMI data conversion techniques for the soil salinity assessment [7–10], the choice of the most suitable approach for each survey is still a challenging task. The uncertainties that emerge with their application depend on a number of site-specific environmental factors, including the complex interactions of soil properties that affect the ECa and distinct data processing requirements, which can significantly impact the credibility of the results. Furthermore, while the technical guidelines and considerations regarding the employment of EM38 in soil salinization surveying have been well documented by existing reviews and scientific publications [11–13], a concise compilation of the currently available approaches that convert ECa measurements by the EM38- and the MK2-type sensors into soil salinity as expressed in ECe has not yet been attempted.

In this respect, the objective of this paper is to provide a comprehensive and up-to-date review of the modeling approaches for monitoring and mapping the saline soils using the EM38 and the MK2 sensors. Through an examination of the approaches and techniques that have been applied for ECe assessment and mapping using the obtained ECa measurements, the aim of this review is to foster a deeper understanding of the sensor's efficiency in the recent and constantly rising demands of detection and monitoring soil salinity.

Specifically, in the following sections:

- The fundamental principles underlying the EM38 and MK2 probes are described, offering thorough insight into their operational mechanisms, capabilities, and constraints.
- Subsequently, the modeling approaches that utilize the EM38 and the MK2 data, for the estimation, prediction, and interpretation of the ECe at different scales, are extensively discussed. The various models and methods that have been developed and convert the sensor's ECa values into ECe are explored, highlighting the most noteworthy considerations regarding their accuracy and reliability.
- Finally, the fusion of the EM38, MK2, and remote sensing data for monitoring and mapping the saline soils is overviewed and followed by a brief summary of conclusions and future directions.

By addressing these aspects, the aim of this review is to enrich the current field of soil salinization research and elaborate on the potential of EM38 and MK2 sensors in the future modeling and assessment of soil salinity and eventually in developing precise management practices that will prevent land degradation and protect resources.

2. Materials and Methods

With the aim of obtaining a comprehensive and up-to-date overview of the modeling approaches that utilize the EM38 and MK2 data, we adopted an in-depth research methodology. Initially, for the collection and the thorough examination of the literature related to our objective, an online search using academic databases and search engines was employed. These included Elsevier Scopus, ScienceDirect, MDPI, as well as Google Scholar. The research criteria and the keywords that were applied in the selected electronic resources were: ("EM38" OR "EM38MK2" OR "EMI") AND ("salinity models" OR "soil salinity") OR ("Remote Sensors" AND "soil salinity"). The types of publications scoped for our review were restricted to those written in English. This encompassed journal articles,

research papers, review papers, book chapters, conference papers, theses, and technical notes related to the principles and characteristics of the EM38 and MK2 sensors.

From searching all the databases, we retrieved a total of more than 300 articles. In order to identify and acquire the most relevant literature from the gathered publications, we reviewed their titles and abstracts. After excluding duplicates and less relevant publications, the remaining articles were full-text reviewed. Ultimately, a total of 170 documents were selected, analyzed, and cited in the present study.

3. Results

3.1. Fundamental Principles and Considerations of the EM38 and MK2 Sensors

3.1.1. Basic Operational Features of EM38 and MK2 Sensors

The deployment of electromagnetic induction (EMI) instruments has been consolidated in agricultural science and soil surveying since the 1970s [14–16]. Owing to their low cost and their capability to detect the spatial variations in edaphic properties and heterogeneities within the field and at larger scales, in real time, and non-destructively [17,18], they have been studied and used for numerous environmental and geophysical applications [12].

Unlike other geophysical methods such as TDR and GPR, the quantification of soil salinity's spatial variations by electrical resistivity (ER) and EMI devices has become a vital component of precision management implementations [11,19]. This is mainly amplified by the measurements of apparent electrical conductivity (ECa), which have been found to be correlated with soil salinity estimates and can be used as an indirect indicator for many soil properties [20]. Frequency domain reflectometry (FDR) technology, including WET sensors, has also been successful in the appraisal of soil salinity in the laboratory [21–23] and in situ [19,24] using ECa measurements. Nevertheless, the single utilization of these probes might be exacting and locally restricted since they have a substantially smaller measurement volume and are invasive, as their operation is based on contact with the soil and its sublayers [24].

Over the years, commercial EMI sensors, such as the DUALEM (Dualem Inc., Milton, ON, Canada), EM31, EM34 (Geonics Ltd., Mississauga, ON, Canada), and Profiler EMP-400 (Geophysical Survey Systems, Inc., Salem, NH, USA) have been investigated for the assessment of various soil properties, including soil salinity, and their performance has been documented [25–27].

The ground conductivity meter EM38 (Geonics Ltd., Mississauga, ON, Canada), introduced in 1980, was revolutionary in soil salinization surveys due to its light weight, portability, and the large volume of ECa measurements taken in various types of soils and fields, e.g., stony, which until then were difficult to acquire with electrode-based devices [28,29]. Thus, it quickly gained the attention of the agricultural community and became the most frequently applied tool for monitoring and mapping soil salinity [20]. The adaptation of EM38 can also be attributed to the fact that it was intentionally designed to support the assessment of near-surface variations in soil properties and specifically of soluble salts that affect crops within the rooting zone [30,31].

The EM8 sensor is constructed with two coils, one transmitter and one receiver coil, which are installed at the opposite ends of the instrument with a fixed spacing of 1 m, and it operates at a 14.6 kHz frequency. The orientation of the coils determines the cumulative depth response of the instrument associated with the ECa measurements. When located in the horizontal configuration (EMh), the device's signal corresponds to a depth range of roughly up to 0.75 m, whereas in the vertical mode (EMv) the penetration depth is approximately up to 1.5 m. The depth range of the instrument sufficiently covers the root volume of most plants [32]. These depth-weighted responses of ECa, however, are theoretical measuring depths that rely on a non-linear function in homogeneous soils. As a result, the absolute depth values cannot be easily defined [33].

Since its release, the EM38 has undergone several modifications, updates, and technical improvements, including the addition of a GPS receiver, which allows for accurate georeferencing of the data, and the development of user-friendly software for data analysis

and visualization. The dual-dipole EM38 DD sensor is an example of these modifications. This version consists of two EM38 units attached together and placed horizontally and vertically for recording simultaneous EMh and EMv measurements [34,35].

In 2008, the EM38MK2 (Geonics Ltd., Mississauga, ON, Canada) was launched as an updated version of the original EM38 instrument [30]. The MK2 type encompasses new attributes and enhancements regarding the depth range response, stability, and facilitations concerning the field survey and data acquisition. Compared to its predecessor, the MK2 has hardware and software that offer more automation in operation, easier processing, and better interpretation of the raw data. In particular, it can simultaneously measure both soil conductivity (Q/P) and magnetic susceptibility (I/P) within two discrete depth ranges. It entails temperature compensation circuitry, which reduces the occurring temperature drifts during the survey, and it supports automatic calibration without laborious adjustments. This can be achieved through a wireless Bluetooth data logger, which enables the collection of the data and the communication with the instrument conveniently from a relative distance. Alternatively, data recording can be performed through a serial port. The duration of field operations has also been enhanced with the addition of a power connector, which allows for the use of an external rechargeable battery [36]. Both instruments are presented in Figure 1.

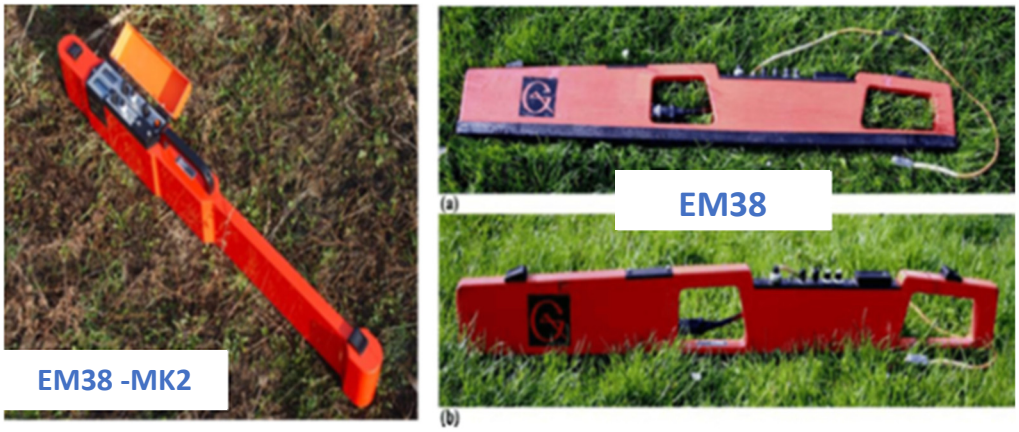

Figure 1. The EM38-MK2 and EM38 devices. (**a**) The EM38 in horizontal mode. (**b**) The EM38 in vertical mode (from Geonics Ltd., Catalano [37] and Siddique [38]).

Besides the technical advancements, the main fundamental difference between the two sensor types lies in the second receiver coil of the MK2, which corresponds to an additional depth range of measurements. The MK2 consists of one transmitter coil and two receiver coils that are positioned at two fixed distances of 1 m and 0.5 m from the transmitter coil, respectively. Hence, in the MK2, the effective depth range is determined by both the coil separation and the dipole modes of horizontal and vertical orientation. Consequently, with the new coil (0.5 m coil separation), measurements of ECa can be additionally taken at two distinct depths: at 0.375 m depth when the device is placed in horizontal mode (EMh) and at 0.75 m in the vertical mode (EMv) (Figure 2). This version allows users to detect and investigate variations in shallower layers, which may be optimal for precise agriculture practices [26,33]. Moreover, along with the rest of the depth ranges of the sensor, the profile of soil salinity distribution up to a 1.5 m depth can be promptly acquired and evaluated.

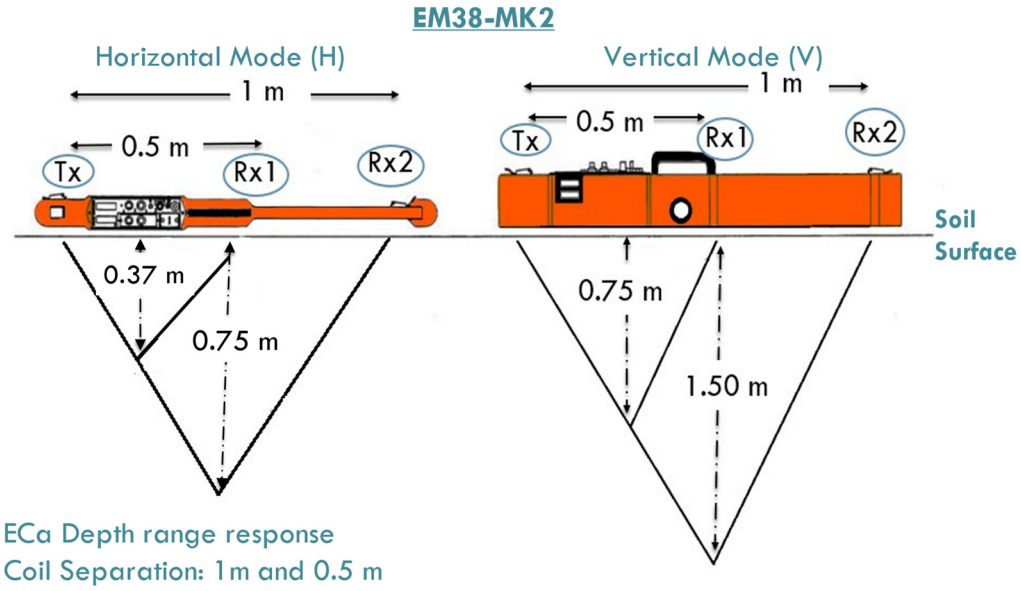

Figure 2. The EM38MK2 sensor in horizontal (H) and vertical (V) mode with the effective depth range responses of ECa for coil separation of 1 m and 0.5 m when placed on the soil surface. T× refers to the transmitter and R × 1, R × 2 to the two receiver coils.

The relative differences, advantages, and applicability of the EM38 and MK2 sensors over various geophysical instruments in mapping of soil properties have been discussed in a few studies [12,26,39,40]. Gebbers et al. [26], by comparing a variety of EMI and other technology devices (ARP03, CM-138, EM38, EM38-DD, MK2, OhmMapper, Veris 3100), concluded that the main disadvantage of EM38, EM38-DD, and CM138 sensors is their sensitivity to deeper soil layers, which is irrelevant to the crop's rootzone. On the other hand, MK2, ARP03, OhmMapper, and Veris3100 were found to be more effective in detecting shallower soil variations that are important for precision agriculture. Likewise, the EM31 and EM34 sensors, which have exploration depths of up to 6 and 60 m, respectively, may also be considered inappropriate for detecting the variability in shallower soil layers [12]. In a study conducted by Dooltitle et al. [39], the use of EM38 and the multifrequency device GEM 300 was investigated, revealing that both sensors provide reasonable estimates of soil salinity. Moreover, Urdanoz et al. [40], by comparing the EM38 and the DUALEM sensor, indicated that although EM38 tends to produce slightly higher horizontal ECa readings than the DUALEM, both sensors can be used interchangeably. Generally, the EMI sensors exhibit close similarities in their collected data, with the main differences attributed to the different operational modes and sensing depths [30].

3.1.2. Principles of the EM38 and MK2 Operation

The operation of the EM38 and MK2 instruments is based on the principles of EMI and has been established by McNeil [41,42]. Once the sensors are turned on and properly calibrated for recording ECa measurements, the transmitter coil sends, at a frequency of 14.6 kHz, an alternating electrical current to the soil, generating a primary magnetic field (H_p). When the primary field interacts with the subsurface, it induces electrical currents (eddy currents) that, in turn, produce secondary magnetic fields (H_s). These secondary fields interact with the receiver coils by inducing alternating currents in the coils. The sum of the amplitude and phase of the induced voltages from the primary and secondary fields is amplified in an output voltage, which is read by the user.

Accordingly, under low induction number (LIN) conditions, where Nb << 1 and assuming homogeneity in the depth profile, the apparent electrical conductivity, ECa, is sensed and expressed as the ratio of the primary (H_p) and the secondary magnetic fields

(H_s) (Equation (1)), where f is the operating frequency (Hz), μ_o, the magnetic permeability of free space ($4\pi 10^{-7}$ H m^{-1}), s is the intercoil spacing (m), and $\omega = 2\pi f$ [41].

$$ECa = \frac{4}{2\pi f \mu_0 s^2}\left(\frac{H_s}{H_P}\right) \quad (1)$$

Besides other factors, ECa readings by the EM38 and MK2 sensors for an investigated depth range are influenced by the orientation and coil spacing of the instruments. The relative ranging depths for the horizontal and vertical modes have been determined by McNeil [41] in homogeneous soils as non-linear functions that describe the relative contribution to the secondary magnetic fields in respect to normalized depth z.

Consequently, the depth-weighted response, which indicates the cumulative depth response R(z) of the sensors, is a non-linear function that represents the relative contributions of all soil electrical conductivities from a soil volume below a normalized depth z. The R(z) equations, based on the horizontal and vertical orientation and expressed as a percentage (%) of the measured signal, have been defined for 1 m (Equations (2) and (3)) and 0.5 m (Equations (4) and (5)) coil separation [33,41]:

$$R_v(z) = \frac{1}{(4z^2+1)^{1/2}} \quad (2)$$

$$R_H(z) = \frac{1}{(4z^2+1)^{1/2}} - 2z \quad (3)$$

$$R_v(z) = \frac{1}{\left(4\left(\frac{z}{0.5}\right)^2+1\right)^{1/2}} \quad (4)$$

$$R_H(z) = \left(4\left(\frac{z}{0.5}\right)^2+1\right)^{1/2} - 2\left(\frac{z}{0.5}\right) \quad (5)$$

where z (m) is the depth and $R_H(z)$ and $R_v(z)$ are the cumulative relative ECa for horizontal and vertical mode, respectively.

From the derived cumulative functions, the depth of investigation (DOI), which refers to the depth from which more than 70% of the signal response derives, can be determined for each sensor. Heil et al. [33] compared the two instruments and examined the effective depth responses for each orientation and coil distance. The coil spacing of 0.5 and the horizontal mode are generally influenced by near-surface variability, making them more suitable for shallower depths. Instead, the 1 m spacing coil and the vertical mode seem to have an increased sensitivity along with the depth. It is noteworthy that the EM38's vertical response decreases drastically at depths above 90 cm, in contrast to MK2. Practically, the DOI of the sensors may vary under natural soil conditions due to existing heterogeneities and the interrelations of ECa with subsurface soil features that affect the signal.

In addition to the effective depth ranges when placed on the ground surface, both devices can be lifted at different heights above the soil surface to investigate interval depth variations and model the distribution of salt content in the soil layers [43–45]. Also, they are designed for handheld measurements or can be mounted on non-metallic sleds and attached to vehicles for mobile measurements. The mobile and real-time collection of ECa data by the EM38 and MK2 sensors is a simple process owing to their software and the direct connection to the GPS. Thus, they can be an ideal option for monitoring and mapping soil salinization at field scales [46–48].

3.1.3. Considerations in the EM38 and EMK2 Applications

One of the key factors in the employment of the EM38 and MK2 sensors is that on all occasions of soil salinity surveying, either at field or larger scales, site-specific calibration is required. Therefore, soil sampling for ground-truth data cannot be omitted [30].

Another important consideration when using these probes for the collection of ECa measurements is their susceptibility to metal and electrical interference, like fences and power lines. In comparison to other technologies, such as capacitance sensors, the presence of metallic objects in the study area can affect the signal, especially in the horizontal configuration [36]. Although the detection of metals may be beneficial for archaeological prospecting [49], for efficient soil salinity estimation and mapping, uniform, metal-free soils are a prerequisite. Furthermore, as the manufacturer recommends, in the automatic mode of ECa recording, more frequent calibrations might be needed to minimize any potential effects from the drifts on the accuracy [50]. The drifts by temperature are stronger in the original EM38 [20,33], while for the MK2, they are considered insignificant due to the internal enhancements. An exception might arise in the case of near-surface measurements with the 0.5 m spacing coil, where the effects from the drifts need to be managed [50].

Finally, one of the most concerning and constraining aspects of EM38's utility for determining solute distribution within the soil is its application under dry moisture conditions or in fields where there is insufficient moisture through the penetration depths. Conducting ECa surveys in fields where soil water content levels are less than those of field capacity and reportedly under 50% [51] can lead to unreliable and biased results. Likewise, ECa measurements in shallow and moderately deep soils above bedrock should be avoided [30,52].

3.2. Modeling Approaches for the Assessment and Mapping of ECe Using the EM38 and MK2 Data

The conventional strategies for the assessment of soil salinity consist of soil sampling and laboratory estimation of the electrical conductivity of saturated paste extract, ECe, which is the standard method. These laborious, costly, and time-consuming methods tend to be impractical for fields and large-scale areas since they are point-based and cannot provide a sufficient number of measurements for extended monitoring [30,53]. The non-invasive, cost-effective, and rapid measurements of ECa by the EM38 and the latest MK2 have become one of the most widely accepted and reliable alternatives for determining the spatiotemporal variation in soil salinity in arid and semi-arid regions [54]. In practice, the main benefit of these EMI instruments is that they allow quick and large numbers of georeferenced ECa measurements, which can be significantly correlated to the spatial variability of soil properties and especially soil salinity, providing information on the soil quality of the croplands [30,55,56]. In addition, the obtained data can be efficiently utilized to generate detailed maps of subsurface property spatial patterns and processes. These high-resolution maps enable the design of field and large-scale sustainable management decisions [10].

ECa is the weighted average of the vertical electrical conductivity distribution within the soil volume as depicted in a one-dimensional (1D) earth model [57]. It is influenced by various physical and chemical soil properties and their interrelations [19]. In this sense, factors such as soil moisture, soil salinity, texture, mineralogy, and temperature affect the EM38 signal and need to be considered when interpreting geospatial ECa measurements with respect to a particular property survey [51,58].

In salt-affected areas where ECa values are higher than 2 ds m^{-1}, the spatial variability of solute concentration has been proven to be the dominant factor contributing to ECa, and the provided soil moisture is close to field capacity across the research district [30,59]. In this instance, EMI measurements can most likely be directly correlated with soil salinity mapping [48]. In non-saline soils and soils with relatively low conductivity levels, however, ECa is strongly related to a function of soil properties, which include soil water content, the amount and type of clay, cation exchange capacity (CEC), organic matter (OM), and soil temperature [20,60–64]. Among them, volumetric water content and clay proportion have been reported as the major factors affecting the values of ECa [61–63,65,66]. In most situations of ECa surveying, soil moisture and soil salinity are considered the most influential factors, whereas the effect of other factors, like soil temperature, is weaker. It

is worth mentioning that the strength of the effect of each soil property on ECa varies depending on specific soil conditions.

The complex relationships between ECa and soil properties have been examined in numerous site-specific management studies and described by various models. The volumetric water content of the soil is the primary pathway for electric current flow [60,67], thus exhibiting a strong positive relationship with ECa. When water content drops below a threshold value, ECa decreases significantly and becomes negligible since the conductance path ceases to exist. Moreover, like soil salinity, water content is considered a dynamic property, meaning that after certain circumstances (e.g., rainfall, nonuniform irrigation applications), it can gradually change across the field and soil profile, complicating the interpretation of its effects on ECa [11]. Similarly, the high concentration of the dissolved salts in the soil solution leads to an increase in ECa readings [60,62]. In non-saline soils, the increase in soil moisture enhances the pathway for current to flow through the soil, resulting in higher values of ECa. The contribution of soil texture to the spatial patterns of ECa varies according to the particle sizes and the charge density of their surface area. ECa values tend to be higher in fine-textured and clay-rich soils due to their larger surface area, which allows them to absorb and retain more ions [62,68]. Conversely, in coarser-textured soils, ECa tends to decrease and exhibit larger variations. Soil texture can influence the water-holding capacity of the soil. Therefore, in uniform cropping systems, soils with high clay and water content are likely to lead to an increase in ECa [60,62]. In conditions with highly spatial texture variations, however, characterizing soil ECa variability becomes difficult [69]. In addition, temperature fluctuations during the survey have a substantial impact on field measurements. Due to the positive temperature dependency of ECa, which increases by almost 2% for every 1 °C temperature rise, ECa readings are recommended to be referenced at 25 °C using corresponding equations [41,64]. Finally, cation exchange capacity (CEC) and organic matter (OM) also show a positive correlation with ECa [62,70]. Overall, various soil properties and their influence on ECa are summarized in Table 1.

Table 1. Different soil factors and their effect on ECa.

Factor	Effect on ECa Values
Water Content	Higher moisture levels increase ECa Dry soils have lower ECa
Soil Salinity	High salinity levels increase ECa
Texture	Clay content: Higher proportion increases ECa Silt, Sand Content: Higher proportion decreases ECa
Temperature	Increasing temperature increases ECa
Cation Exchange Capacity (CEC)	Higher CEC increases ECa
Organic Matter (OM)	Higher percentage increases ECa

The depth-weighted average conductivity of ECa does not indicate the distribution of the actual salt concentration with depth in the soil profile but rather reflects the average cumulative response of the sensor, weighted according to respective soil depths [41,42]. Thus, a modeling approach to establish a relationship between ECa measurements and true salinity levels like ECe, or EC1:5, at various depths is necessary for the prediction and monitoring of soil salinization across different spatial and temporal scales. The conversion of the EM38 data for soil salinity analysis encompasses a variety of simple or more advanced statistical and mathematical procedures, integration with data and sources from other technologies, as well as spatial modeling techniques. Among these, the preferred modeling approach can be applied to estimate, predict, and map the soil salinity profile, leading to precise rootzone management and mitigation of salinization impacts.

Based on the land use, the size of the study area (e.g., plot [71], field [7], landscape [72], regional [10], urban greenery [73]), and the purpose of the salinity survey, several approaches applying the EM38 and MK2 sensors have been reported for assessing soil salinity in terms of ECe and displaying its spatiotemporal characteristics.

3.2.1. Deterministic and Stochastic Conversion of ECa

One of the initial considerations in the assessment of ECe using an EM38 sensor depends upon the conversion of ECa through a stochastic or deterministic approach [70,74,75].

ECe values can be deterministically predicted from the in situ ECa data using geophysical models that have been developed based on the laws of EMI response to saturated or unsaturated conditions [12,76]. In this non-geostatistical approach, ECa readings are converted into ECe through theoretically or empirically determined formulas that incorporate physicochemical soil characteristics estimated or measured within the study area [35]. Well-established models such as Archie's 1942 model [77] and the dual pathway parallel conductance (DPPC) of Rhoades et al. [67,78] describe the ECa as a multiplicative function of soil parameters under different porous media and soil circumstances. These and other similar models [79] have been broadly examined for the detection and estimation of water and solute concentrations in the soil profile.

While deterministic models acknowledge the significance of the complex interactions between ECa and soil properties, their application in soil salinization monitoring is limited by their static nature. The requirement for precise information on additional soil properties such as soil water content or texture and the dynamic process of soil salinity, varying over space and time, makes this approach suitable mostly for local and short-term simulations [80,81].

An alternative method to overcome the challenges in interpreting the spatiotemporal variations in ECe with EM38 measurements is the stochastic or geostatistical approach [35]. This modeling technique relies on the correlation of ECa data with ECe for the direct prediction of soil salinity. This involves using soil sampling and geostatistical or spatial regression models. During the ECa survey, a number of soil samples are collected from the measurement points and analyzed to determine the corresponding ECe. The paired set of ECe and ECa values is then used to establish an ECe = f (ECa) relationship with the aid of regression and geostatistical analysis. Subsequently, this developed calibration equation is applied to predict the ECe values from the remaining non-sampled ECa measurements [7,82].

The site-specific calibration between ECe and the simultaneous EM38 or MK2 measurements, as a necessity for the accurate appraisal and mapping of soil salinity, has been the center of attention in numerous studies [7,8,83–86]. Over the past decades, the calibration of ECa data has been extensively explored and improved at field and local scales due to advancements in geostatistics and data processing tools. However, uncertainties in the generated maps of soil salinity still emerge from the employment of these techniques [87]. Furthermore, monitoring the spatial and temporal trends of soil salinity at a regional scale demands continuous data and calibration parameters from different fields, which may not always be available or easily accessible [88,89].

Geostatistical methods have been indispensable tools in soil salinity monitoring and mapping, as they are applied to model and predict the spatiotemporal variability in large salt-affected areas. Based on the spatial dependence and structure of the georeferenced variables, techniques like kriging and variogram modeling offer the advantage of predicting ECe values at unsampled locations [90], with relatively high accuracy [91]. They require dense soil sampling with approximately more than 50 sampling points to ensure reliable calibration with minimum errors [92]. Therefore, their application is not recommended for field surveys [91].

Spatially referenced regression models, on the other hand, have gained great recognition due to their simplicity and the reduced need for soil sampling [53]. They are regression equations with optional trend surface variables that assume an independent underlying error structure. This error is related to the variations between ECa and estimated ECe values. Despite their benefits, as regards their predictive efficacy, they cannot reach the same degree of accuracy as the geostatistical models [7,93]. Nonetheless, the regression modeling approach yields viable results in most cases of regional scales [94,95]; hence, it remains one of the most appealing and preferable calibration techniques.

These approaches are also adopted when applying ECa-directed soil sampling for soil salinity mapping [11,35,51]. According to this concept, when a correlation between measurements and soil salinity exists, geospatial ECa measurements can be used to construct a directed sampling plan for the selection of the optimal soil sampling sites. This method is accomplished either deterministically, through design-based sampling schemes, or stochastically with model-based sampling designs.

Based on ECa-directed soil sampling, in fields where salinity is not the dominant soil property influencing the EM38 measurements, the variations in ECa can act as a surrogate for identifying the site locations that depict an adequate range and variability of the soil salinity. The soil samples collected from these particular sites can then serve as ground-truth data for the accurate calibration of ECa to ECe. The calibration model, in turn, results in producing spatially reliable maps of soil salinity across multiple scales [48]. In saline soils with uniform texture and water content conditions, however, the ECa variation is mainly attributed to salt concentration; thus, it can be used as a soil salinity indicator.

The overall process of ECa-directed sampling for mapping the spatial distribution of soil salinity may be expedited by the available commercial software packages. The ECe Sampling Assessment and Prediction (ESAP) developed in USDA [96] is a conductivity modeling software, which based on a response-surface sampling design, may generate the minimum set of sampling points needed for the calibration of the EM38 measurements to ECe. Additionally, it embraces both deterministic and stochastic methods for the prediction of the spatial ECe values from the ECa survey data [71]. To date, several researchers have used the ESAP programs with EM38 readings as a tool to delineate and map ECe distribution at irrigated fields [71,97–99] and district scales [100]. Amezketa [71], using customized ESAP software and EM38 data, assessed and displayed the spatial patterns of soil salinity at an irrigated plot in Spain. The accuracy of the developed models for the multiple-depth ECe values ranged from $R^2 = 0.38$ in the topsoil (0–30 cm) to $R^2 = 0.90$ in the subsurface (30–60 cm). Also, based on the selected calibration models, the average ECe profile (0–90 cm) was mapped. Slimane et al. [100], after obtaining EM38 readings from a 240 ha region of Tunisia, imported the data into the ESAP to determine the appropriate soil sampling locations and to estimate and map the spatial variability of the area's ECe. According to the study's results, the average R^2 of the prediction models for different soil depths was approximately 0.78, ($0.6 \leq R^2 \leq 0.8$) and the ECe variation maps showed that salinity increased with depth.

Besides this general classification, the most common and current modeling approaches for the conversion of EM38 and MK2 data into soil salinity are listed below. Each of these models includes techniques that can be applied individually or in combination to achieve the specific objectives they are intended for. Essentially, simple regression techniques could be appropriate for ECe estimation in the field, but for mapping the spatiotemporal variability of ECe in irrigated regional districts, more sophisticated procedures might be necessary. The purpose of conducting a salinity survey with EM38-type sensors, whether qualitative or quantitative, is of major importance in defining the level of accuracy and the modeling approach to be utilized [101]. The following section focuses on the diverse approaches that address the conversion of raw EM38 and MK2 data into ultimate ECe values and their representations across a variety of scales and applications, as documented in the existing literature. The categorization of the available modeling approaches serves as a means to comprehend their fundamental characteristics and techniques and explore the range of their consistency and weaknesses. It is important to note that the types of models presented in the study are not rigidly distinct but may share common attributes. The various categories are designed to provide guidance and facilitate the identification of areas where the methods of soil salinity appraisal and mapping can be enhanced.

3.2.2. Regression-Based Models (Linear, MLR, Simple Depth-Weighted Coefficients, Established Coefficients, Modeled Coefficients, Mathematical Coefficients)

The earliest studies that were carried out for soil salinity assessment using the EM38 probe were entirely based on producing sets of regression equations and searching for calibration coefficients for a specified range of depths at the site of interest. In order to detect the salinity distribution within the field, the weighted ECa data are transformed to determine the ECe profile by fitting linear or non-linear regression models at depth intervals and calculating the coefficients for each depth range. This framework involves the development of empirical calibrations relating the instrument's horizontal and vertical observations, either separately or in combination, to ECa measured with a probe at known depth intervals [102–104]. The predicted equations of the probe's ECa can then be reconstructed to estimate the soil ECe. Alternatively, equations are developed to directly relate the sensor's measurements to a single weighted ECe value [83,105] or ECe at different depth increments. Typically, in these approaches, the vertical profiling of ECe is derived through a one- or two-step process that leverages the operational dipole modes of the sensor and depends on the establishment of regression relationships between the obtained and the ground-truth conductivity data. They utilize the field EM38 readings, taken on the soil surface or at distinct heights above it, to define the ECa layering and the collection of soil samples from corresponding depth increments for the construction of calibration models [106].

The various published calibration model functions that have been retrieved mainly through linear (LR) [83] and multiple linear (MLR) regression analysis [71,84,85,107] include known approaches such as depth-weighted coefficients [105]; established coefficients, which are empirical-mathematical coefficients [108,109]; modeled coefficients [103]; mathematical coefficients based on the theoretical EMI depth response function [110]; and the logistic profile model [85]. Johnston et al. [111] compared several of the developed calibration approaches to evaluate their performance in soil salinity estimation. As they reported, the established coefficients of Corwin and Rhoades [108,109] and the modeled coefficients of Slavich [103], which predict the probe ECa, exhibited results with low bias but with significant errors. Also, the depth-weighted coefficients model of Wollenhaupt et al. [105], which determines the weighted ECe, was observed to perform poorly with high error values (RMSE = 5.33). Furthermore, Triantafilis et al. [85] indicated that the logistic profile, which consists of a mixed nonlinear model, can provide smoother and less erratic prediction profiles than the established coefficients and the multiple-regression coefficients model [104].

The common trait of the proposed models and approaches is that they all use regression parameters that are site-specific and time-dependent to a significant degree [112]. Hence, they will not perform at the same level of accuracy when applied in dissimilar soil conditions to those they have been developed in. The fluctuations in the prediction results can be attributed to the variations in soil volumetric water content and soil texture across different locations [111,113] and to misleading homogeneous assumptions [85]. This arises from the fact that the calibrations of ECa measurements are being established, assuming that soil salinity is the only soil property affecting the response of the EM38, thus excluding the influence of other soil factors in the equation. In these instances, a strong relationship between EM38 data and ECe values can be confirmed [12]. Additionally, since most of these calibration models rely on linear equations, they use a best fit line through the data, usually an ordinary least-squares (OLS) regression, a technique that is accompanied by certain attributes. This prediction method is associated with key assumptions such as the normality and independence of errors and homoscedasticity for obtaining valid coefficients [93,114]. Therefore, deviations from meeting these criteria can compromise the reliability of the coefficients and result in inaccurate predictions and potentially biased conclusions for the salt-affected area.

3.2.3. Geostatistical Models

The comprehension and characterization of soil salinity spatial distribution constitutes a fundamental element of the sustainable management practices and prevention of soil salinization [7,115,116]. Due to the need for high spatial resolution data and expanding coverage, determining and mapping the spatial variations in soil salinity at the land and regional scales by soil sampling appears unfeasible [30,117].

In contrast, this process can be accomplished by using the EM38 and MK2 instruments and performing spatial predictions at the field and land scales [30,55]. The promptly collected ECa data can be employed with geostatistical methods, enabling the quantification and interpretation of the spatial variability of ECe over large areas [118,119]. Soil salinity severity maps may also be generated to support the proper decision-making for crop and land management [120].

The geostatistical models, in the context of conversion, refer to a set of geostatistical methods and tools, such as interpolation and variogram analysis, which are implemented as a means of modeling, predicting, and mapping the spatial variations [92] of soil salinity from the sensor's data. The geostatistical processes can be carried out by appropriate software packages.

More specifically, the models are constructed to analyze the spatial patterns of the data and also predict values for the variable at unsampled locations, diminishing the weakness of point measuring from proximal sensing and creating a constant spatial coverage [73,121]. Considering the scientific concern and practical constraints in characterizing the distribution of soil salt in a continuous space, the contribution of geostatistics, which identifies the spatial variation structure and predicts unsampled data, is significant.

The analysis, definition, and quantification of the variance structure of soil salinity can be achieved with variogram calculations, whereas the prediction of the spatial variability of ECe for generating informative salinity maps is obtained with an interpolation method.

The spatial prediction and mapping of ECe, based on geostatistics, can be potentially adopted in two different ways. The ECa measurements can be initially interpolated for the prediction of unsampled ECa values, and the amount of spatial ECa data can then be calibrated for the estimation of ECe and eventually analyzed with a variogram. This approach has proven to have controversial results depending on the interpolation method and the density of the EM38 data [8,119].

The second and most established method prioritizes the prediction of ECe by developing a relationship between ECa measurements and ECe values, usually with linear regression analysis [94,122,123]. Thereafter, variogram analysis and interpolation techniques can be applied to the predicted ECe for mapping and evaluating the spatial patterns of soil salinity across the study area. The accuracy of this modeling approach depends on various factors that need to be taken into account. Aside from ensuring the quality of the EM38 data, the primary aspect is associated with the selection of the interpolation technique and the distinct sampling design that they require [7]. In a similar sense, the sampling scheme is essential for the reliability of the variograms [92]. Moreover, different and more sophisticated approaches than linear regression for calibrating ECa data might perform with higher accuracy [120].

To date, there is a diversity of geostatistical interpolation methods available, several of which have been examined and compared using the EM38 and MK2 sensors for the prediction and mapping of the spatial variability of ECe at the landscape [124], district [8,120], and regional scales [94,123]. They extend from basic kriging to more contemporary tools, such as ordinary kriging [123], universal kriging, and hybrid interpolation techniques that integrate different technologies, like regression kriging, co-kriging [7], indicator kriging [122], or 3D kriging [94]. All geospatial procedures, including variogram analysis, interpolation methods, and spatial data visualization, can be executed with commercially available software packages, such as Geostatistics Software GS+ [123], Golden Software Surfer [97], ESRI ArcGIS [122] and ArcMap [120], and Geo R [82]. Yet, despite the variety of these spatial estimation tools, there has not been a single optimal method reported for

the interpolation of the data [73]. For example, Jantaravikorn et al. [120], after identifying a strong ECa–ECe correlation for both modes of EM38 (r = 0.86 and r = 0.87), examined the accuracy of four distinct spatial interpolation methods for soil salinity prediction on categorized validation datasets using ESRI ArcMap and SAGA software. The predicted horizontal and vertical ECa data were then classified to create soil salinity severity maps. ordinary co-kriging was found to be an accurate interpolation method for predicting soil salinity when using the horizontal data of the sensor (R^2 = 0.85), while the deterministic inverse distance weighting (IDW) was found to be more suitable for the vertical mode (R^2 = 0.83).

The applicability of these methods has been investigated mostly for the prediction and interpretation of the spatial distribution of soil salinity at a point in time. Recently, Xie et al. [123], based on ECa data using the MK2 and the geostatistical methods of semivariograms and ordinary kriging, which were conducted with the aid of Geostatistics Software (GS + 7.0) and ArcMap 10.2, respectively, quantified and interpreted the spatiotemporal distribution and variations in regional soil salinity across several years. The satisfactory results of the linear prediction model, which was conducted with ECa measurements for the topsoil ($R^2 > 0.90$), indicate the use of the MK2 in the assessment and mapping of the spatiotemporal variability of soil salinity and foster the potential for further applications under similar soil conditions.

In the field, changes in solute distribution on a spatial and temporal scale have been characterized and evaluated in three dimensions using the MK2 and the non-geostatistical interpolation method of inverse distance weighting (IDW) [125]. In this work, multivariate linear models were established for the relationship of ECe with ECa in various soil layers and times. The predicted ECe values were then interpolated using the deterministic 3D IDW technique. Besides the high model reliability ($0.82 < R^2 < 0.99$), the 3D IDW was also proven to predict the three-dimensional spatiotemporal variations in soil salinity with good accuracy and R^2 values ranging from 0.76 to 0.77.

Regardless of the option of a deterministic or geostatistical interpolation method, mapping the spatiotemporal characteristics of solute distribution by the geostatistical modeling approach comes with certain limitations. The existence of a strong relationship between ECe and ECa measurements is a basic requirement [11]. In addition, the accumulation of high-quality data following specific distributional assumptions for the prediction of unsampled values is necessary. Finally, since these methods are based on the spatial dependence of the variables, they may not be suitable for processing and predicting more complex and non-spatial relationships.

3.2.4. Inversion Models

Monitoring and mapping of the vertical extent of salinity within the soil profile using the EM38 probes has been remarkably improved by the inversion approach [126]. Inversion modeling is an evolving and steadily increasing applied process for the estimation and mapping of depth-specific soil salinity from EMI data [48,127]. It consists of various complex algorithms and calculation methods that enable the conversion of the recorded ECa data to depth-specific estimates of electrical conductivity. The inverted data are then modeled using calibration techniques for the prediction of ECe at any depth [128,129] or depth increments [130], and the production of multidimensional (1D, 2D, 3D) maps of the salinity profile for the investigated district [131]. The rapid and efficient assessment of solute distribution with depth is essential for acquiring an accurate and real-time quantitative interpretation of the salt dynamics in the profile and especially in the rootzone [112,132].

Recently, the growing interest in inversion procedures for the spatiotemporal analysis of soil salinity has been associated with the development of multi-coil (e.g., CMD-Mini Explorer) and multi-frequency (e.g., GEM 2) EMI sensors, which are designed to take simultaneous measurements at multiple depth ranges [132–134]. However, the cost and limited access to these instruments [126] make the application of EM38 and MK2 an attractive alternative.

Several inversion approaches that employ EM38 data have been explored for modeling the vertical patterns of solutes. Some of the initial attempts were linear [135] and non-linear models [136], which included the Tikhonov regularization to invert the ECa data. The data in these cases were obtained by taking multi-height EM38 measurements in the horizontal and vertical orientations at different sites. Second-order Tikhonov regularization is a mathematical method suggested for reducing possible data errors and stabilizing the inversion process. It is applied as a technique to overcome the "ill-posedness" and the "non-uniqueness" that are encountered in the inversion. These problems entail measurement or data errors that can induce significant changes in the outcome and the fact that there might be more than one solution for different ECa profiles [117,137]. In addition to these issues, the 1D inversion models, as mentioned above, though applicable, characterize only the vertical distribution with depth, thus providing limited information on the actual transfer of salt within the soil profile [131,138].

Other approaches, in order to predict the estimates of soil salinity in discrete soil layers, joined the EM38 measurements with ECa data from different EMI sensors, like the EM31 [139] or EM34 [140], and inverted them with a 1D algorithm with 2D smoothness constraints to display the vertical and lateral variations in soil salinity in the subsurface along transects [139]. Moghadas et al. [141] proposed a joint inversion of the horizontal and vertical EM38 data using a probabilistic optimization algorithm. The derived one-dimensional inversion models were merged to generate a 3D image of the subsurface distribution of soil salinity at a regional scale. To evaluate the robustness of the models, the inverted data were calibrated to ground-truth ECe values using linear regression for certain depths. As observed, the models exhibited a good prediction (R^2 = 0.67) for the shallow layers (30 cm), while for the deeper soil layers (60, 90 cm) the discrepancies were attributed to the high clay content of the study area.

The efficient models that have been developed during the last decade rely on advanced inversion strategies that can extract 2D or 3D electromagnetic conductivity images (EMCIs) of the spatial distribution of soil salinity from the ECa data [131]. Software packages like EM4Soil have been released to assist in the process of inversion of ECa data directly in 1D [72], 2D [128,142,143], or quasi-3D [126,129] layered conductivity values and generate EMCIs by applying inversion parameters. The prediction of ECe from the inverted EM38 readings can be achieved with high accuracy by establishing simple calibration equations, such as linear regression (LR) [128–130]. Farzamian et al. [126], addressing the need for affordable and easily accessible monitoring tools as an alternative to non-available multi-coil instruments, proposed the use of multi-height EM38 data and a quasi-3D inversion algorithm for the development of ECe maps in the landscape. They indicated that by collecting multiple ECa measurements at different heights, a single regional calibration equation (LR) instead of discrete depth-specific calibrations may predict the ECe at any desired depth.

By these means, detailed maps of the spatial patterns of ECe across various depths in large and landscape-irrigated areas can be efficiently produced. Also, the quasi-3D inversion models of ECe can be combined with remote sensing to create a 3D map and illustrate the quantitative and qualitative spatial distribution of soil salinity in the survey area [130]. The application of inverse modeling to the three-dimensional distribution of soil salinity is an important evolutionary step for characterizing and interpreting the lateral and vertical variations within the soil profile. This contribution might be particularly prominent in mapping the local 3D patterns of the solutes variability in more complicated irrigation schemes, such as micro-irrigation systems [99].

Moreover, the temporal distribution of soil salinity with depth has been examined most recently by using time-lapse inversion of ECa measurements with multiconfiguration systems [132,144,145]. Time-lapse inversion of ECa data by EM38 and MK2 instruments is a challenging approach that has not been investigated for soil salinity assessment [146,147] and only with a strictly limited scope for moisture content distribution, which involves measurements from the electrical resistivity tomography (ERT) [145,146,148]. The difficulty

is ascribed to the complex dynamics of solutes, which can vary significantly within the soil profile. Therefore, the method requires multiple local soil data and measurements to be repeated over time for the determination of the solute's temporal trend [48]. A recent attempt has been made by Paz et al. [127], who collected repeated measurements by the EM38 sensor at specific locations and dates and inverted them to obtain time-lapse EMCIs of the vertical profiling of the layered estimates of electrical conductivity. By using a pre-constructed calibration model of ECe for the same area, the layered conductivity estimates were converted to predict ECe. The prediction model was found to be adequately precise (R^2 = 0.88) in depicting the spatiotemporal variations in soil salinity with depth and across the study area.

While the inversion modeling approach yields positive outcomes in the spatiotemporal mapping of soil salinity, it should be mentioned that the credibility and the accuracy of its application depend on the quality of the acquired data and regularization factors [148]. Therefore, thorough validation using datasets independent of those employed in the prediction process is pivotal for minimizing uncertainties in the results [127] and ensuring the credibility of the survey. Furthermore, when using time-lapse inversion at regional scales, the establishment of precise local-specific calibrations needs to be taken into account. High temporal variations in dynamic soil properties, such as water content, can have a substantial impact on the assessment of the solute variations and consequently misdirect soil treatment decisions [127].

3.2.5. Machine-Learning-Based Models

Lately, a new modeling approach has been introduced for characterizing and quantifying the spatial variations and depth distribution of soil salinity with data from EM38 and MK2 devices. This encompasses the integration of ECa measurements, remote sensing data, and environmental variables with machine-learning (ML) technology to generate digital soil maps (DSMs) of ECe in large arid zones [4,52,149,150]. According to this approach, the prediction and mapping of salt-affected areas can be substantially improved when proximal sensed data and multi-spectral information from remote sensing imagery are incorporated [54], and advanced machine-learning algorithms are utilized to assess and model the relationship of ECe with these multiple variables [4,150].

Plenty of modeling methods have been elaborated and extensively used in DSM applications for various soil properties [151], including soil salinity. However, advanced methods that utilize various machine-learning algorithms with EMI and the EM38 and MK2 probes in particular for the prediction of soil salinity are currently being explored. The growing interest in machine-learning modeling is attributed to its ability to process huge volumes of datasets and identify the complex and non-linear interactions between soil properties and various environmental features [152]. For soil salinity assessment, the models use a composite of statistical and mathematical formulas through which they capture and "learn" the relationship between the spatial variations in ECa data and input variables. After successful training, they can predict the unknown spatial patterns of soil salinity at large scales [4].

Contrary to geostatistical models, machine-learning models employ a more computational operation for the prediction of soil salinity's spatial variability. While geostatistical modeling relies on the spatial dependency structure of the data, machine-learning-based models use algorithms that detect the relations and patterns between soil properties and the variables.

There are many machine-learning algorithms available for the prediction and digital mapping of soil properties, with varying principles, complexity, and overall performance. Some of them include decision trees (DTs), random forest (RF), support vector machines (SVMs), genetic programming (GP), and artificial neural networks (ANNs). Among them, random forest has been proven to be a reliable and robust option for developing prediction models of soil salinity and producing explicit digital soil maps, particularly in arid areas [10]. Ding et al. [4], based on the dipole mode of the portable MK2, established a

random forest model with ECa measurements, auxiliary variables from remote sensing, and environmental products for predicting the spatial variations in different land types of the oasis agroecosystems in China. The good relationship between the horizontal and vertical ECa data with ECe at all depth increments indicated ECa as a valid predictor for modeling the spatial variations in soil salinity. The application of random forest models with ECa measurements and auxiliary data was found to have high accuracy, with R^2 ranging from 0.77 to 0.84 for all coil configurations. Furthermore, according to the results for various land uses, the derived RF prediction models of ECa seemed to perform better for the deeper soil layers and the bare lands, with an R^2 range from 0.84 to 0.91. Slightly different results for all depth intervals ($0.61 < R^2 < 0.65$) were demonstrated in the same regional area when RF models of ECe were constructed with the involvement of MK2 measurements and remote sensing imagery as covariates [150].

Owing to the implementation of machine-learning-based models with the use of the MK2 probe, fine-resolution maps of soil salinity in large areas may be produced [150,153]. Moreover, the magnitude of influence the diverse soil, environmental, or other site-related variables have in the prediction of soil salinity can easily be exhibited and evaluated [149]. Their capability to provide complex non-linear interrelations between soil properties and a vast amount of existing data without making any distributional assumptions may offer great opportunities in future surveys of soil salinity mapping.

Despite the inspiring benefits, their application is associated with practical weaknesses. The prediction of subsurface soil salinity using machine-learning techniques is primarily driven by the diverse variables that are utilized as inputs for their training. Thus, collecting and employing accurate and relevant attributes from the available resources require some level of data expertise. Also, given that the efficiency of these models depends on the quality of the input data, there cannot be a unique algorithm for assessing the spatial and temporal variability of soil salinity in all soil and site circumstances with the same accuracy.

3.2.6. Hybrid Models

The nature of soil salinity comprises alterations over time and space. The diverse changes, which extend from the complex distribution in the rootzone to spatial variations across the field and larger scales, are crucial to determine in order to interpret and control the sources of soil salinization. These issues, however, need to be reconciled with rapid and resilient methods, as precise irrigation systems and soil sustainability strategies at the regional and global levels are imperative. The application of individual modeling techniques like simple regression-based models may fail to adapt to all these requirements. To this end, hybrid models have emerged, which combine different methods and data sources for estimating and mapping the spatial variations in soil salinity at different scales [101].

The hybrid modeling approach is presented as a broader category of models that encompasses the integration of multiple techniques with data obtained by proximal EM38 and MK2 devices and additional data mainly derived from remote sensing.

These models incorporate geostatistical, machine learning, and empirical methods to leverage the strengths and advantages of each approach and overcome the constraints or weaknesses that they might have as individual models in soil salinity assessment [154]. Particularly for the detection and mapping of the spatial distribution of solutes within the profile and across a large area, the hybrid models based on EM38, MK2, and remote sensing data integrate advanced hybrid geostatistical techniques like regression kriging with machine-learning algorithms, such as random forest or Cubist. This fusion of approaches and data sources can identify and predict the complex relationships of solutes with different variables within the profile and, at the same time, determine the soil salinity's spatial variations in the study area.

This innovative and promising modeling approach could potentially lead to more accurate predictions of spatiotemporal patterns of soil salt content and eventually to a better understanding and representation of soil salinity dynamics at a regional level. To

date, however, few studies have examined its efficiency in monitoring and mapping soil salinity using the EM38 and MK2 probes.

The hybrid modeling approach of Taghizadeh-Mehrjardi et al. [149] combined remote sensing and MK2 data with hybrid geostatistical methods and machine learning. They applied regression kriging for the spatial prediction and digital mapping of horizontal and vertical ECa using auxiliary data at certain depth intervals. Then, the advanced machine-learning algorithm Cubist (regression tree) was applied to the set of variables to model the spatial distribution of ECe values at the standard depths. As they documented, the prediction models of ECe in the arid region of Arkadan had varying accuracy ($0.11 < R^2 < 0.78$), with the spatial distribution performing better in the upper soil (0–30 cm).

Another hybrid approach for modeling and mapping the spatial variations in soil salinity is the combination of multi-spectral data from high-resolution remote imagery with measurements from the MK2 and the use of partial least-squares regression (PLSR) [101]. As was reported, the constructed spectral-PLSR-based prediction models could reliably ($R^2 = 0.67$) detect and monitor the variations in soil salinity in the oasis region of the Keriya River in China.

In an attempt to explore methods for integrating new sources of soil data as inputs in DSMs, Zare et al. [52] compared three approaches using MK2 measurements and ECe data collected from a region near the saline Maharlu Lake in Iran. They concluded that the approach involving the combination of machine learning, quantile random forest model, and regression co-kriging on the residuals, with R^2 values up to 0.79, can be effectively used for the prediction of ECe. Also, the MK2 data were found to be a reliable and meaningful input for digitally mapping the soil salinity variations, especially in cases where there is a lack of appropriate remote sensing data.

Nonetheless, the hybrid modeling approach, in order to be applicable, requires a correlation between the input variables. Specifically for generating soil salinization maps, a strong relationship between ECa measurements and ground-truth data of ECe needs to be valid. In addition, the selection of the appropriate modeling techniques according to the existing survey data plays a significant role in the reliability and accuracy of the results [154].

A summary of the documented modeling approaches for the assessment and mapping of soil salinity by the EM38 and MK2 measurements is presented in Table 2. Each modeling approach is accompanied by the various techniques or methods that have been employed within it. Referenced studies for each case are also shown for further exploration.

3.3. Fusion of the EM38, MK2, and Remote Sensing Data for Soil Salinity Monitoring and Mapping

To mitigate the global impacts of soil salinization, there is an urgent need to retrieve accurate information on its status in arid and semi-arid regions quickly and consistently. This has prompted researchers to gradually develop more robust approaches that integrate multiple data and technologies to interpret the changes in soil salt content and preserve the agricultural sustainability of the irrigated systems in these areas [155,156]. In the last few years, these efforts have focused on the combination of remote sensing data with ground-based EMI sensors for complementary and potentially high-precision monitoring and mapping of soil salinity variability at different scales [1,54,56,149,157].

Remote sensing, by providing repetitive, current, and prompt high-resolution images like those of WorldView 2, has become a valuable tool for identifying and mapping the solutes' spatiotemporal variations across the surface of large and severely saline areas [158,159]. The capability, however, of the available multi-spectral satellite data is restricted to the detection and assessment of surface soil salinity [160], disregarding the three-dimensional spatial distribution of salt content in the soil profile. Moreover, spectral reflectance can be problematic in regions with slightly low to moderate salinity levels and limited or no visible salt features due to interference from other site factors, such as vegetation cover or soil type [159,161].

Table 2. Short summary of the modeling approaches and methods that have been used for the assessment and mapping of soil salinity in terms of ECe using EM38 or EM38 MK2 measurements, at different scales.

Model	Methods	Reference Studies
Regression-Based (Calibration Models)	Linear, multiple linear	[104,107]
	Simple depth-weighted coefficients	[105]
	Established coefficients	[108,109]
	Modeled coefficients	[103]
	Mathematical coefficients	[110]
Geostatistical	Interpolation methods (OK [1], CO-K [2], OCK [3], universal kriging, indicator kriging, 3D kriging) Semi/variogram analysis	[8,94,98,120,122,123]
Deterministic Spatial Interpolation	3D IDW	[125]
Inversion	Tikhonov regularization	[135,136]
	Joint inversion	[72,139,141]
	2D algorithms	[128,142,143]
	Quasi-3D algorithms	[126,129]
Machine-Learning-Based	Random forest	[4,150]
Hybrid	Cubist (ML), regression kriging	[149]
	Partial least-squares regression, spectral index	[101]
	Quantile random forest (ML), regression co-kriging	[52]

[1] OK: ordinary kriging, [2] CO-K: co-kriging, [3] OCK: ordinary co-kriging.

On the contrary, the EM38 and MK2 sensors have been broadly employed and evaluated for the quantification and characterization of soluble salt distribution within the subsurface and the rootzone. The fusion of EM38 and MK2 field measurements with multi-temporal [162,163] and multi-spectral [73,101,124,150] remote sensing datasets has been documented in a few soil salinity surveys, which vary from agricultural and urban greenery systems to different soil crops, irrigation schemes, and scales. In most circumstances, particularly in bare lands and large arid or semi-arid areas, it has been suggested as an effective, inexpensive, and time-efficient method for predicting and monitoring the spatiotemporal variations in soil salinity with relative accuracy [54,101,149,163].

For instance, Wu et al. [162], based on acquired MK2 field measurements and ECe from soil sampling, used multi-temporal remote sensing (vegetation indices) data to develop salinity models of the severely salinized region of Dujaila in Iraq. The derived multi-year maxima-based models, which were applied for mapping and tracking the spatiotemporal changes in the salt-affected areas, achieved high accuracy in predicting soil salinity, with R^2 reaching a value of 82.5. Vegetation indices such as the NDVI that are utilized in remote sensing tend to become a significant innovative tool for mapping the entire rootzone salinity at the regional scale and potentially in the field and landscape as well [48]. However, they need to be calibrated. Thus, even though the process of ground-truth data collection can be considerably reduced owing to the MK2 measurements [52], it remains a necessity for appropriate field calibration [160]. Ding and Yu [54] constructed regression models using EM38 readings and various spectral indices from satellite images for the prediction and evaluation of seasonal and spatial variations in soil salinity in the Delta Oasis of the Tarim Basin, China. They also examined three interpolation techniques for assessing the distribution patterns of salt concentration within the region. According to their findings, the fusion of EM38 data with salinity indices from remote sensing images can provide the assessment of salinity at a regional scale for both dry and wet seasons with fairly high

accuracy. Moreover, the results indicate the importance of EM38 measurements in designing rapidly and simply the most suitable soil sampling strategy for the survey. Additional soil sampling is needed for the interpolation's accuracy. Among universal kriging, spectral index regression, and regression kriging, the regression kriging with nested spherical model was found to have the closest fit to the measured ECa ($R^2 > 0.90$).

On other occasions, however, the combination of the sensors seems to need further research. By employing an EM38 sensor and using data from remote sensing, Nouri et al. [73] investigated the soil salinity in urban greenery spaces of the Adelaide Parklands in Australia. In order to predict the variations in solutes at different spatial and temporal scales, regression models for the EM38 were developed with various vegetation and salinity indices from high-resolution satellite images. The EM38 data were validated with ECe values from soil samples. As the authors observed, although the soil-adjusted vegetation index (SAVI) was found to be a good predictor, the proximal sensor was considered more efficient than the spectral indices in predicting soil salinity in urban landscapes in semi-arid climates. Additionally, Gharsallah et al. [124] observed that, in large arid lands that are densely planted, such as an irrigated olive orchard, multivariate models of EM38 data with soil spectral indices from low-resolution images may exhibit poor accuracy in predicting and mapping the soil salinity distribution ($R^2 < 0.12$). Nonetheless, in these models, the integration of vegetation indices and high-resolution images may resolve the influence of the dense tree canopy on the remote sensing reflectance and improve the overall reliability [124].

The fusion of field EM38 and MK2 data with remote sensing techniques, including high-quality satellite data and selected indicators like vegetation indices, can contribute to more thorough and concordant maps of soil salinity. Monitoring the spatial and temporal distribution of solutes through field EMI surveys and remote sensing can be sufficiently accomplished without excessive soil sampling. This can accelerate the understanding of soil salinization severity at multiple scales and lead to rapid remediation measures.

4. Discussion

From the results of the research, it was observed that the approaches utilizing the EM38 and MK2 data for soil salinity assessment and mapping have been centered around regression-based (calibration) models, geostatistical methods, deterministic interpolation methods, inversion models, machine-learning algorithms, and hybrid modeling.

According to the reviewed literature, the developed calibration models exhibit limited applicability since they use entirely site-specific equations and regression coefficients that cannot be accurately applied in different locations [48,85,111,112]. Moreover, these models rely on distributional and subsurface homogeneous assumptions, which exclude from their equations the impact of influential soil properties, such as soil texture and soil water content, on ECa measurements [63]. Nevertheless, linear regression can be employed as a viable, easy, and simple calibration technique in conjunction with the geostatistical [94,122,123] and the inversion [126–130] modeling approaches. The geostatistical models have contributed significantly to the prediction and interpretation of soil salinity spatial variations over the years. With a diversity of classic and more advanced interpolation methods available, they have been proven to provide relatively accurate estimations of ECe on a range of soil scales [94,120,123]. However, since their application depends on the spatial structure of the collected data, their solitary use is not suggested in circumstances where more complex and non-spatial relationships among the variables need to be assessed. As was observed from the findings, the inversion modeling approach has gained wide acceptance in the scientific community, and its applications in salinity surveys using the EM38 and MK2 sensors are increasing and evolving. The benefit of these methods lies in the easy conversion of multiple ECa measurements through software to determine ECe at different depths and generate detailed multidimensional (2D, 3D) images of the soil salinity profile with high accuracy [118–120,126,128,142,143]. Besides the variety of studies that characterize the spatial variations using the EM38 and MK2, recent studies have made efforts to assess

the temporal variability of solutes, yielding good results [127]. In all cases, the inversion prediction models require rigorous validation with independent datasets to be credible [127]. Machine-learning-based models have also emerged as a powerful approach in the current field of soil salinity monitoring and mapping. Their capability to process immense amounts of data and capture complex, non-linear interrelations between the sensor's ECa data and a plethora of input variables is considered their major advantage over other modeling techniques. The findings from the literature demonstrated that the implementation of machine-learning techniques combined with MK2 data, auxiliary data from remote sensing, and environmental variables can predict with significant accuracy the spatial and temporal variability of soluble salts on the large scale of arid zones and generate fine-resolution maps [4,52,149,150]. Recently, an increasing number of studies have focused on developing such integrating approaches and coupling them with hybrid techniques of geostatistical interpolation and machine learning. These approaches have been found to produce reliable soil salinity predictions and DSMs, particularly in the arid regions of the world [52,149], but caution is needed in the selection of the proper techniques. In a similar sense, the review's findings highlighted the fusion of the EM38 and MK2 data with high-quality satellite data and vegetation indices from remote sensing as an effective, rapid, and promising method for the prediction and mapping of the spatiotemporal variations in soil salinity in large arid areas [54,101,149,162,163].

5. Conclusions and Future Directions

By exploring the latest modeling approaches for the assessment and mapping of soil salinity using the EM38 and MK2 sensors, we attempted to enrich and enhance the current research field of soil salinization monitoring and mitigation through this review. Specifically, through a comprehensive summary of the applied approaches and methods, the paper intended to elucidate and underline the role of EM38 and MK2 in the detection and interpretation of soil salinity and facilitate researchers and users in making well-informed decisions concerning future salinity surveys and agricultural treatments.

The advantage of the EM38 and MK2 sensors in soil salinity surveys is their capability to collect rapid and effortlessly numerous field ECa measurements that can be conveniently related to soil salinity, especially in high-salt-affected areas. By applying simple or more sophisticated modeling approaches, the ECa data can be converted to salinity estimates of ECe, revealing valuable insights into the spatiotemporal patterns and depth distribution of solutes at various scales and land types. Due to the complicated interactions of soil salinity with various soil properties and factors and its continuous changes over time and space, the measurements by EM38 and MK2 sensors are pivotal for the subsurface mapping of saline soils in a timely manner. The enhanced ground conductivity meter MK2, which is easy to operate and cost-effective compared to the latest multi-coil sensors, can be significantly useful in subsurface salinity mapping, especially in cases where other soil data sources, such as remote sensing, are unavailable.

To date, despite the research and technological progress, there is not a universally approved and applicable modeling approach for the assessment and monitoring of soil salinization. Therefore, the construction of efficient salinity models using the EM38 and MK2 probes should be carried out considering the available approaches and their adaptation under different soil and environmental conditions. It is essential to have a full understanding of the current modeling options and their techniques so the optimal method can be selected and the spatiotemporal characteristics of the salt-affected areas can be accurately identified and interpreted.

In this sense, by using the sensor's field readings at various depths and employing an inverse modeling technique, the spatial and temporal variability of soil salinity at large irrigated farms can be predicted and quantified in 3D maps. This enables the detailed monitoring of soil salt variations within the field and the design of proper soil management practices. Moreover, advanced approaches like hybrid models, which combine EM38 and MK2 readings with multiple site-specific datasets and methods like machine learning and

interpolation, may overcome the limitations of single model applications and increase the accuracy of ECe predictions. Subsequently, the interpretation of the complex soil salinity dynamics across the study area can be fulfilled. Finally, the recent trend of integrating georeferenced EM38 and MK2 measurements with remote sensing data indicates great opportunities in delineating the soil salinity distribution within the rooting zone and across large arid regions. This approach can improve the implementation of precise and timely sustainable strategies and substantially reduce the need for excessive soil sampling.

Consequently, further exploration of such promising methods at multiple scales is crucial for generating reliable and up-to-date salinity maps. More attention should be directed toward extending and validating the inverse modeling at a regional scale and in distinct irrigation systems to create consistent 3D maps of the spatiotemporal variability of soil salinity. In addition, efforts to incorporate machine-learning algorithms with multi-period remote sensing data, auxiliary variables, and EMI data should be intensified to track and map the long-term variations in soluble salt depositions at the regional level, refine the method, and expand it toward global-scale predictions. Furthermore, a deeper investigation of the diverse environmental, topographic data, and spectral indices as covariates is needed to identify and optimize the predictor variables of soil salinity mapping in different soil conditions and cultivation systems.

Ultimately, the validation of robust, sophisticated approaches that combine field measurements using sensors like the EM38MK2 and contemporary technologies can potentially minimize the time, labor, and cost of ground-truth data and render a fundamental basis for the efficient prediction and real-time monitoring of soil salinization at the field, regional, and global scales.

Author Contributions: Conceptualization, G.K. and P.A.P.; methodology, P.A.P.; validation, G.K. and P.A.P.; formal analysis, P.A.P.; investigation, P.A.P.; resources, P.A.P.; data curation, P.A.P.; writing—original draft preparation, P.A.P.; writing—review and editing, P.A.P.; visualization, G.K. and P.A.P.; supervision, G.K.; project administration, G.K. and P.A.P. All authors have read and agreed to the published version of the manuscript.

Funding: This research received no external funding.

Data Availability Statement: Not applicable.

Conflicts of Interest: The authors declare no conflict of interest.

References

1. Corwin, D.L. Climate Change Impacts on Soil Salinity in Agricultural Areas. *Eur. J. Soil Sci.* **2021**, *72*, 842–862. [CrossRef]
2. Besma, Z.; Christian, W.; Didier, M.; Pierre, M.J.; Mohamed, H. Soil Salinization Monitoring Method Evolution at Various Spatial and Temporal Scales in Arid Context: A Review. *Arab. J. Geosci.* **2021**, *14*, 283. [CrossRef]
3. Scudiero, E.; Corwin, D.; Anderson, R.; Yemoto, K.; Clary, W.; Wang, Z.; Skaggs, T. Remote Sensing Is a Viable Tool for Mapping Soil Salinity in Agricultural Lands. *Calif. Agric.* **2017**, *71*, 231–238. [CrossRef]
4. Ding, J.; Yang, S.; Shi, Q.; Wei, Y.; Wang, F. Using Apparent Electrical Conductivity as Indicator for Investigating Potential Spatial Variation of Soil Salinity across Seven Oases along Tarim River in Southern Xinjiang, China. *Remote Sens.* **2020**, *12*, 2601. [CrossRef]
5. Goldshleger, N.; Ben-Dor, E.; Lugassi, R.; Eshel, G. Soil Degradation Monitoring by Remote Sensing: Examples with Three Degradation Processes. *Soil Sci. Soc. Am. J.* **2010**, *74*, 1433–1445. [CrossRef]
6. Rodrigues, H.M.; Vasques, G.M.; Oliveira, R.P.; Tavares, S.R.L.; Ceddia, M.B.; Hernani, L.C. Finding Suitable Transect Spacing and Sampling Designs for Accurate Soil ECa Mapping from EM38-MK2. *Soil Syst.* **2020**, *4*, 56. [CrossRef]
7. Lesch, S.M.; Strauss, D.J.; Rhoades, J.D. Spatial Prediction of Soil Salinity Using Electromagnetic Induction Techniques: 1. Statistical Prediction Models: A Comparison of Multiple Linear Regression and Cokriging. *Water Resour. Res.* **1995**, *31*, 373–386. [CrossRef]
8. Triantafilis, J.; Odeh, I.O.A.; McBratney, A.B. Five Geostatistical Models to Predict Soil Salinity from Electromagnetic Induction Data Across Irrigated Cotton. *Soil Sci. Soc. Am. J.* **2001**, *65*, 869–878. [CrossRef]
9. Aboelsoud, H.; Abdel-Rahman, M. Rapid Field Technique for Soil Salinity Appraisal in North Nile Delta Using EM38 through Some Empirical Relations. *Int. J. Plant Soil Sci.* **2017**, *14*, 1–9. [CrossRef]
10. Wang, F.; Shi, Z.; Biswas, A.; Yang, S.; Ding, J. Multi-Algorithm Comparison for Predicting Soil Salinity. *Geoderma* **2020**, *365*, 114211. [CrossRef]
11. Corwin, D.L.; Scudiero, E. Field-scale Apparent Soil Electrical Conductivity. *Soil Sci. Soc. Am. J.* **2020**, *84*, 1405–1441. [CrossRef]

12. Heil, K.; Schmidhalter, U. The Application of EM38: Determination of Soil Parameters, Selection of Soil Sampling Points and Use in Agriculture and Archaeology. *Sensors* **2017**, *17*, 2540. [CrossRef] [PubMed]
13. Heil, K.; Schmidhalter, U. Theory and Guidelines for the Application of the Geophysical Sensor EM38. *Sensors* **2019**, *19*, 4293. [CrossRef] [PubMed]
14. Williams, B.; Baker, G. An Electromagnetic Induction Technique for Reconnaissance Surveys of Soil Salinity Hazards. *Soil Res.* **1982**, *20*, 107. [CrossRef]
15. De Jong, E.; Ballantyne, A.K.; Cameron, D.R.; Read, D.W.L. Measurement of Apparent Electrical Conductivity of Soils by an Electromagnetic Induction Probe to Aid Salinity Surveys. *Soil Sci. Soc. Am. J.* **1979**, *43*, 810–812. [CrossRef]
16. Nogués, J.; Robinson, D.A.; Herrero, J. Incorporating Electromagnetic Induction Methods into Regional Soil Salinity Survey of Irrigation Districts. *Soil Sci. Soc. Am. J.* **2006**, *70*, 2075–2085. [CrossRef]
17. Abdu, H.; Robinson, D.A.; Jones, S.B. Comparing Bulk Soil Electrical Conductivity Determination Using the DUALEM-1S and EM38-DD Electromagnetic Induction Instruments. *Soil Sci. Soc. Am. J.* **2007**, *71*, 189–196. [CrossRef]
18. De Benedetto, D.; Castrignanò, A.; Rinaldi, M.; Ruggieri, S.; Santoro, F.; Figorito, B.; Gualano, S.; Diacono, M.; Tamborrino, R. An Approach for Delineating Homogeneous Zones by Using Multi-Sensor Data. *Geoderma* **2013**, *199*, 117–127. [CrossRef]
19. Kargas, G.; Londra, P.A.; Sotirakoglou, K. Evaluation of Soil Salinity Using the Dielectric Sensor WET-2. *Soil Res.* **2022**, *61*, 397–409. [CrossRef]
20. Sudduth, K.A.; Drummond, S.T.; Kitchen, N.R. Accuracy Issues in Electromagnetic Induction Sensing of Soil Electrical Conductivity for Precision Agriculture. *Comput. Electron. Agric.* **2001**, *31*, 239–264. [CrossRef]
21. Krishan, G.; Kumar, R.; Suresh; Gopal, K.; Saha, S.K. Measuring Soil Salinity with WET Sensor and Characterization of Salt Affected Soils. *Agropedology* **2008**, *18*, 124–128.
22. Kargas, G.; Persson, M.; Kanelis, G.; Markopoulou, I.; Kerkides, P. Prediction of Soil Solution Electrical Conductivity by the Permittivity Corrected Linear Model Using a Dielectric Sensor. *J. Irrig. Drain. Eng.* **2017**, *143*, 04017030. [CrossRef]
23. Kargas, G.; Kerkides, P. Determination of Soil Salinity Based on WET Measurements Using the Concept of Salinity Index. *J. Plant Nutr. Soil Sci.* **2018**, *181*, 600–605. [CrossRef]
24. Visconti, F.; De Paz, J.M. Field Comparison of Electrical Resistance, Electromagnetic Induction, and Frequency Domain Reflectometry for Soil Salinity Appraisal. *Soil Syst.* **2020**, *4*, 61. [CrossRef]
25. Huang, J.; Koganti, T.; Santos, F.A.M.; Triantafilis, J. Mapping Soil Salinity and a Fresh-Water Intrusion in Three-Dimensions Using a Quasi-3d Joint-Inversion of DUALEM-421S and EM34 Data. *Sci. Total Environ.* **2017**, *577*, 395–404. [CrossRef] [PubMed]
26. Gebbers, R.; Lück, E.; Dabas, M.; Domsch, H. Comparison of Instruments for Geoelectrical Soil Mapping at the Field Scale. *Near Surf. Geophys.* **2009**, *7*, 179–190. [CrossRef]
27. Khongnawang, T.; Zare, E.; Srihabun, P.; Triantafilis, J. Comparing Electromagnetic Induction Instruments to Map Soil Salinity in Two-Dimensional Cross-Sections along the Kham-Rean Canal Using EM Inversion Software. *Geoderma* **2020**, *377*, 114611. [CrossRef]
28. Rhoades, J.D. Electrical Conductivity Methods for Measuring and Mapping Soil Salinity. In *Advances in Agronomy*; Sparks, D.L., Ed.; Academic Press: Cambridge, MA, USA, 1993; Volume 49, pp. 201–251. [CrossRef]
29. Hendrickx, J.M.H.; Baerends, B.; Raza, Z.I.; Sadig, M.; Chaudhry, M.A. Soil Salinity Assessment by Electromagnetic Induction of Irrigated Land. *Soil Sci. Soc. Am. J.* **1992**, *56*, 1933–1941. [CrossRef]
30. Doolittle, J.A.; Brevik, E.C. The Use of Electromagnetic Induction Techniques in Soils Studies. *Geoderma* **2014**, *223–225*, 33–45. [CrossRef]
31. Bennett, D.L.; George, R.J. Using the EM38 to Measure the Effect of Soil Salinity on Eucalyptus Globulus in South-Western Australia. *Agric. Water Manag.* **1995**, *27*, 69–85. [CrossRef]
32. Domsch, H.; Giebel, A. Estimation of Soil Textural Features from Soil Electrical Conductivity Recorded Using the EM38. *Precis. Agric.* **2004**, *5*, 389–409. [CrossRef]
33. Heil, K.; Schmidhalter, U. Comparison of the EM38 and EM38-MK2 Electromagnetic Induction-Based Sensors for Spatial Soil Analysis at Field Scale. *Comput. Electron. Agric.* **2015**, *110*, 267–280. [CrossRef]
34. Saey, T.; Van Meirvenne, M.; Vermeersch, H.; Ameloot, N.; Cockx, L. A Pedotransfer Function to Evaluate the Soil Profile Textural Heterogeneity Using Proximally Sensed Apparent Electrical Conductivity. *Geoderma* **2009**, *150*, 389–395. [CrossRef]
35. Corwin, D.L.; Lesch, S.M. Application of Soil Electrical Conductivity to Precision Agriculture: Theory, Principles, and Guidelines. *J. Agron.* **2003**, *95*, 455–471. [CrossRef]
36. EM38-MK2-Operating-Manual.Pdf. Available online: https://geophysicalequipmentrental.com/files/2020/01/EM38-MK2-Operating-Manual.pdf (accessed on 30 August 2023).
37. Catalano-Measuring Soil Conductivity with Geonics Limited E.Pdf. Available online: https://adamchukpa.mcgill.ca/gwpss/Presentations/GWPSS_2011_Catalano.pdf (accessed on 1 October 2023).
38. Siddique, M.N.A. Potential of Soil Sensor (EM38) Measurements for Soil Fertility Mapping. Master's Thesis, Ghent University, Brussel, Belgium, 2020.
39. Doolittle, J.; Petersen, M.; Wheeler, T. Comparison of Two Electromagnetic Induction Tools in Salinity Appraisals. *J. Soil Water Conserv.* **2001**, *56*, 257–262.

40. Urdanoz, V.; Aragüés, R. Comparison of Geonics EM38 and Dualem 1S Electromagnetic Induction Sensors for the Measurement of Salinity and Other Soil Properties: Comparison of Geonics EM38 and Dualem 1S Sensors. *Soil Use Manag.* **2012**, *28*, 108–112. [CrossRef]
41. McNeill, J.D. *Electromagnetic Terrain Conductivity Measurement at Low Induction Numbers: Mississauga. Ontario, Canada*; Technical Note TN-6; Geonics Ltd.: Mississauga, ON, Canada, 1980; Volume 6.
42. Bonomi, E.; Manzi, C.; Pieroni, E.; Deidda, G.P. *Inversion of EM38 Electrical Conductivity Data*; II International Workshop on Geo-Electro-Magnetism (Proccedings), Lerici, Italy, 26–28 September 2001; Accademia Lunigianese di Scienze G. Capellini: La Spezia, Italy, 2001.
43. Yao, R.-J.; Yang, J.-S.; Wu, D.-H.; Xie, W.-P.; Gao, P.; Wang, X.-P. Geostatistical Monitoring of Soil Salinity for Precision Management Using Proximally Sensed Electromagnetic Induction (EMI) Method. *Environ. Earth Sci.* **2016**, *75*, 1362. [CrossRef]
44. Korsaeth, A. Height above Ground Corrections of EM38 Readings of Soil Apparent Electrical Conductivity. *Acta Agric. Scand. B Soil Plant Sci.* **2006**, *56*, 333–336. [CrossRef]
45. Song, J.H. Assessment of the Accuracy of a Soil Salinity Model for Shallow Groundwater Areas in Xinjang Based on Electromagnetic Induction. *Appl. Ecol. Environ. Res.* **2019**, *17*, 10037–10057. [CrossRef]
46. Kitchen, N.R.; Sudduth, K.A.; Drummond, S.T. Mapping of Sand Deposition from 1993 Midwest Floods with Electromagnetic Induction. *J. Soil Water Conserv.* **1996**, *51*, 336–340. Available online: https://www.ars.usda.gov/ARSUserFiles/50701000/cswq-0111-kitchen.pdf (accessed on 31 August 2023).
47. Urdanoz, V.; Amezketa Lizarraga, E.; Clavería, I.; Ochoa, V.; Aragües Lafarga, R. Mobile and Georeferenced Electromagnetic Sensors and Applications for Salinity Assessment. *Span. J. Agric. Res.* **2008**, *6*, 469. [CrossRef]
48. Corwin, D.L.; Scudiero, E. Review of Soil Salinity Assessment for Agriculture across Multiple Scales Using Proximal and/or Remote Sensors. *Adv. Agron.* **2019**, *158*, 1–130. [CrossRef]
49. Dalan, R.A. Defining Archaeological Features with Electromagnetic Surveys at the Cahokia Mounds State Historic Site. *Geophysics* **1991**, *56*, 1280–1287. [CrossRef]
50. Grellier, S.; Florsch, N.; Camerlynck, C.; Janeau, J.L.; Podwojewski, P.; Lorentz, S. The Use of Slingram EM38 Data for Topsoil and Subsoil Geoelectrical Characterization with a Bayesian Inversion. *Geoderma* **2013**, *200–201*, 140–155. [CrossRef]
51. Corwin, D.L.; Lesch, S.M. Protocols and Guidelines for Field-Scale Measurement of Soil Salinity Distribution with EC_a -Directed Soil Sampling. *J. Environ. Eng. Geophys.* **2013**, *18*, 1–25. [CrossRef]
52. Zare, S.; Abtahi, A.; Fallah Shamsi, S.R.; Lagacherie, P. Combining Laboratory Measurements and Proximal Soil Sensing Data in Digital Soil Mapping Approaches. *Catena* **2021**, *207*, 105702. [CrossRef]
53. Brevik, E.C.; Fenton, T.E.; Lazari, A. Soil Electrical Conductivity as a Function of Soil Water Content and Implications for Soil Mapping. *Precis. Agric.* **2006**, *7*, 393–404. [CrossRef]
54. Ding, J.; Yu, D. Monitoring and Evaluating Spatial Variability of Soil Salinity in Dry and Wet Seasons in the Werigan–Kuqa Oasis, China, Using Remote Sensing and Electromagnetic Induction Instruments. *Geoderma* **2014**, *235–236*, 316–322. [CrossRef]
55. Corwin, D.L. Past, Present, and Future Trends of Soil Electrical Conductivity Measurement Using Geophysical Methods. In *Handbook of Agricultural Geophysics*; CRC Press: Boca Raton, FL, USA, 2008.
56. Ren, D.; Wei, B.; Xu, X.; Engel, B.; Li, G.; Huang, Q.; Xiong, Y.; Huang, G. Analyzing Spatiotemporal Characteristics of Soil Salinity in Arid Irrigated Agro-Ecosystems Using Integrated Approaches. *Geoderma* **2019**, *356*, 113935. [CrossRef]
57. Moghadas, D.; Behroozmand, A.A.; Christiansen, A.V. Soil Electrical Conductivity Imaging Using a Neural Network-Based Forward Solver: Applied to Large-Scale Bayesian Electromagnetic Inversion. *Appl. Geophys.* **2020**, *176*, 104012. [CrossRef]
58. Friedman, S.P. Soil Properties Influencing Apparent Electrical Conductivity: A Review. *Comput. Electron. Agric.* **2005**, *46*, 45–70. [CrossRef]
59. Corwin, D.L.; Lesch, S.M. Apparent Soil Electrical Conductivity Measurements in Agriculture. *Comput. Electron. Agric.* **2005**, *46*, 11–43. [CrossRef]
60. Rhoades, J.D.; Raats, P.A.C.; Prather, R.J. Effects of Liquid-phase Electrical Conductivity, Water Content, and Surface Conductivity on Bulk Soil Electrical Conductivity. *Soil Sci. Soc. Am. J.* **1976**, *40*, 651–655. [CrossRef]
61. Brevik, E.C.; Fenton, T.E. Influence of Soil Water Content, Clay, Temperature, and Carbonate Minerals on Electrical Conductivity Readings Taken with an EM-38. *Soil Horiz.* **2002**, *43*, 9. [CrossRef]
62. Kachanoski, R.G.; Wesenbeeck, I.J.V.; Gregorich, E.G. Estimating Spatial Variations of Soil Water Content Using Non-Contacting Electromagnetic Inductive Methods. *Can. J. Soil Sci.* **1988**, *68*, 715–722. [CrossRef]
63. Visconti, F.; De Paz, J.M. Sensitivity of Soil Electromagnetic Induction Measurements to Salinity, Water Content, Clay, Organic Matter and Bulk Density. *Precis. Agric.* **2021**, *22*, 1559–1577. [CrossRef]
64. Sheets, K.R.; Hendrickx, J.M.H. Noninvasive Soil Water Content Measurement Using Electromagnetic Induction. *Water Resour. Res.* **1995**, *31*, 2401–2409. [CrossRef]
65. McCutcheon, M.C.; Farahani, H.J.; Stednick, J.D.; Buchleiter, G.W.; Green, T.R. Effect of Soil Water on Apparent Soil Electrical Conductivity and Texture Relationships in a Dryland Field. *Biosyst. Eng.* **2006**, *94*, 19–32. [CrossRef]
66. Farahani, H.J.; Buchleiter, G.W.; Brodahl, M.K. Characterization of Apparent Soil Electrical Conductivity Variability in Irrigated Sandy And Non-Saline Fields In Colorado. *Trans. ASABE* **2005**, *48*, 155–168. [CrossRef]
67. Rhoades, J.D.; Manteghi, N.A.; Shouse, P.J.; Alves, W.J. Soil Electrical Conductivity and Soil Salinity: New Formulations and Calibrations. *Soil Sci. Soc. Am. J.* **1989**, *53*, 433–439. [CrossRef]

68. McKenzie, R.C.; George, R.J.; Woods, S.A.; Cannon, M.E.; Bennett, D.L. Use of the Electromagnetic-Induction Meter (EM38) as a Tool in Managing Salinisation. *Hydrogeol. J.* **1997**, *5*, 37–50. [CrossRef]
69. Heil, K.; Schmidhalter, U. Characterisation of Soil Texture Variability Using the Apparent Electrical Conductivity at a Highly Variable Site. *Comput. Geosci.* **2012**, *39*, 98–110. [CrossRef]
70. Rhoades, J.D.; Corwin, D.L.; Lesch, S.M. Geospatial Measurements of Soil Electrical Conductivity to Assess Soil Salinity and Diffuse Salt Loading from Irrigation. In *Geophysical Monograph Series*; Corwin, L., Loague, K., Ellsworth, R., Eds.; American Geophysical Union: Washington, DC, USA, 1999; Volume 108, pp. 197–215. [CrossRef]
71. Amezketa Lizarraga, E. Soil Salinity Assessment Using Directed Soil Sampling from a Geophysical Survey with Electromagnetic Technology: A Case Study. *Span. J. Agric. Res.* **2007**, *5*, 91. [CrossRef]
72. Huang, J.; Mokhtari, A.R.; Cohen, D.R.; Monteiro Santos, F.A.; Triantafilis, J. Modelling Soil Salinity across a Gilgai Landscape by Inversion of EM38 and EM31 Data: Modelling Salinity in Gilgai by EM Inversion. *Eur. J. Soil Sci.* **2015**, *66*, 951–960. [CrossRef]
73. Nouri, H.; Chavoshi Borujeni, S.; Alaghmand, S.; Anderson, S.; Sutton, P.; Parvazian, S.; Beecham, S. Soil Salinity Mapping of Urban Greenery Using Remote Sensing and Proximal Sensing Techniques; The Case of Veale Gardens within the Adelaide Parklands. *Sustainability* **2018**, *10*, 2826. [CrossRef]
74. Lesch, S.M.; Corwin, D.L.; Robinson, D.A. Apparent Soil Electrical Conductivity Mapping as an Agricultural Management Tool in Arid Zone Soils. *Comput. Electron. Agric.* **2005**, *46*, 351–378. [CrossRef]
75. Edeh, J.A. Quantifying Spatio-Temporal Soil Water Content Using Electromagnetic Induction. Ph.D. Thesis, University of the Free State, Bloemfontein, South Africa, 2017. Available online: http://hdl.handle.net/11660/6471 (accessed on 22 July 2023).
76. Herrero, J.; Pabuayon, I.L. The Problem with "Apparent Electrical Conductivity" in Soil Electromagnetic Induction Studies. *Adv. Agron.* **2021**, *165*, 161–173. [CrossRef]
77. Archie, G.E. The Electrical Resistivity Log as an Aid in Determining Some Reservoir Characteristics. *Trans. Am. Inst. Min.* **1942**, *146*, 54–62. [CrossRef]
78. Rhoades, J.D.; Loveday, J. Salinity in Irrigated Agriculture. In *American Society of Civil Engineers, Irrigation of Agricultural Crops*; Stewart, B.A., Nielsen, D.R., Eds.; Monograph, American Society of Agronomists: Madison, WI, USA, 1990; Volume 30, pp. 1089–1142.
79. Mualem, Y.; Friedman, S.P. Theoretical Prediction of Electrical Conductivity in Saturated and Unsaturated Soil. *Water Resour. Res.* **1991**, *27*, 2771–2777. [CrossRef]
80. Lesch, S.M.; Corwin, D.L. Using the Dual-Pathway Parallel Conductance Model to Determine How Different Soil Properties Influence Conductivity Survey Data. *J. Agron.* **2003**, *95*, 365–379. [CrossRef]
81. Hassani, A.; Azapagic, A.; Shokri, N. Predicting Long-Term Dynamics of Soil Salinity and Sodicity on a Global Scale. *Proc. Natl. Acad. Sci. USA* **2020**, *117*, 33017–33027. [CrossRef] [PubMed]
82. Corwin, D.L.; Carrillo, M.L.K.; Vaughan, P.J.; Rhoades, J.D.; Cone, D.G. Evaluation of a GIS-Linked Model of Salt Loading to Groundwater. *J. Environ. Qual.* **1999**, *28*, 471–480. [CrossRef]
83. McKenzie, R.C.; Chomistek, W.; Clark, N.F. Conversion of Electromagnetic Inductance Readings to Saturated Paste Extract Values In Soils For Different Temperature, Texture And Moisture Conditions. *Can. J. Soil Sci.* **1989**, *69*, 25–32. [CrossRef]
84. Lesch, S.M.; Rhoades, J.D.; Lund, L.J.; Corwin, D.L. Mapping Soil Salinity Using Calibrated Electromagnetic Measurements. *Soil Sci. Soc. Am. J.* **1992**, *56*, 540–548. [CrossRef]
85. Triantafilis, J.; Laslett, G.M.; McBratney, A.B. Calibrating an Electromagnetic Induction Instrument to Measure Salinity in Soil under Irrigated Cotton. *Soil Sci. Soc. Am. J.* **2000**, *64*, 1009–1017. [CrossRef]
86. Bouksila, F.; Persson, M.; Bahri, A.; Berndtsson, R. Electromagnetic Induction Prediction of Soil Salinity and Groundwater Properties in a Tunisian Saharan Oasis. *Hydrol. Sci. J.* **2012**, *57*, 1473–1486. [CrossRef]
87. Akramkhanov, A.; Brus, D.J.; Walvoort, D.J.J. Geostatistical Monitoring of Soil Salinity in Uzbekistan by Repeated EMI Surveys. *Geoderma* **2014**, *213*, 600–607. [CrossRef]
88. Harvey, O.R.; Morgan, C.L.S. Predicting Regional-Scale Soil Variability Using a Single Calibrated Apparent Soil Electrical Conductivity Model. *Soil Sci. Soc. Am. J.* **2009**, *73*, 164–169. [CrossRef]
89. Corwin, D.L.; Lesch, S.M. Validation of the ANOCOVA Model for Regional-scale EC_a to EC_e Calibration. *Soil Use Manag.* **2017**, *33*, 178–190. [CrossRef]
90. Trangmar, B.B.; Yost, R.S.; Uehara, G. Application of Geostatistics to Spatial Studies of Soil Properties. *Adv. Agron.* **1986**, *38*, 45–94. [CrossRef]
91. Corwin, D.L.; Lesch, S.M. Characterizing Soil Spatial Variability with Apparent Soil Electrical Conductivity. *Comput. Electron. Agric.* **2005**, *46*, 103–133. [CrossRef]
92. Oliver, M.A.; Webster, R. *Basic Steps in Geostatistics: The Variogram and Kriging*; SpringerBriefs in Agriculture; Springer International Publishing: Cham, Switzerland, 2015. [CrossRef]
93. De Caires, S.A.; St Martin, C.; Wuddivira, M.N.; Farrick, K.K.; Zebarth, B.J. Predicting Soil Depth in a Humid Tropical Watershed: A Comparative Analysis of Best-Fit Regression and Geospatial Models. *Catena* **2023**, *222*, 106843. [CrossRef]
94. Liu, G.; Li, J.; Zhang, X.; Wang, X.; Lv, Z.; Yang, J.; Shao, H.; Yu, S. GIS-Mapping Spatial Distribution of Soil Salinity for Eco-Restoring the Yellow River Delta in Combination with Electromagnetic Induction. *Ecol. Eng.* **2016**, *94*, 306–314. [CrossRef]
95. Corwin, D.L.; Lesch, S.M. A Simplified Regional-Scale Electromagnetic Induction—Salinity Calibration Model Using ANOCOVA Modeling Techniques. *Geoderma* **2014**, *230–231*, 288–295. [CrossRef]

96. Lesch, S.M.; Rhoades, J.D.; Corwin, D.L. *ESAP-95 Version 2.01R: User Manual and Tutorial Guide*; USDA-ARS; George, E.B., Jr., Ed.; Salinity Laboratory: Riverside, CA, USA, 2000.
97. Ganjegunte, G.; Leinauer, B.; Schiavon, M.; Serena, M. Using Electro-Magnetic Induction to Determine Soil Salinity and Sodicity in Turf Root Zones. *J. Agron.* **2013**, *105*, 836–844. [CrossRef]
98. Narjary, B.; Meena, M.D.; Kumar, S.; Kamra, S.K.; Sharma, D.K.; Triantafilis, J. Digital Mapping of Soil Salinity at Various Depths Using an EM38. *Soil Use Manag.* **2019**, *35*, 232–244. [CrossRef]
99. Corwin, D.L.; Scudiero, E.; Zaccaria, D. Modified Eca–ECe Protocols for Mapping Soil Salinity under Micro-Irrigation. *Agric. Water Manag.* **2022**, *269*, 107640. [CrossRef]
100. Ben Slimane, A.; Bouksila, F.; Selim, T.; Joumada, F. Soil Salinity Assessment Using Electromagnetic Induction Method in a Semi-Arid Environment—A Case Study in Tunisia. *Arab. J. Geosci.* **2022**, *15*, 1031. [CrossRef]
101. Kasim, N.; Tiyip, T.; Abliz, A.; Nurmemet, I.; Sawut, R.; Maihemuti, B. Mapping and Modeling of Soil Salinity Using WorldView-2 Data and EM38-KM2 in an Arid Region of the Keriya River, China. *Photogramm. Eng. Remote Sens.* **2018**, *84*, 43–52. [CrossRef]
102. Corwin, D.L.; Rhoades, J.D. Establishing Soil Electrical Conductivity—Depth Relations from Electromagnetic Induction Measurements. *Commun. Soil Sci. Plant Anal.* **1990**, *21*, 861–901. [CrossRef]
103. Slavich, P. Determining ECa-Depth Profiles from Electromagnetic Induction Measurements. *Soil Res.* **1990**, *28*, 443. [CrossRef]
104. Rhoades, J.D.; Corwin, D.L. Determining Soil Electrical Conductivity-Depth Relations Using an Inductive Electromagnetic Soil Conductivity Meter. *Soil Sci. Soc. Am. J.* **1981**, *45*, 255–260. [CrossRef]
105. Wollenhaupt, N.C.; Richardson, J.L.; Foss, J.E.; Doll, E.C. A Rapid Method For Estimating Weighted Soil Salinity from Apparent Soil Electrical Conductivity measured with An Aboveground Electromagnetic Induction Meter. *Can. J. Soil Sci.* **1986**, *66*, 315–321. [CrossRef]
106. Vlotman, W.F.; Chaudhry, M.R.B.A. *Electromagnetic Induction Device (EM38) Calibration and Monitoring Soil Salinity/Environment (Pakistan)*; ILRI: New Delhi, India, 2000; pp. 37–48.
107. Slavich, P.; Petterson, G. Estimating Average Rootzone Salinity from Electromagnetic Induction (EM-38) Measurements. *Soil Res.* **1990**, *28*, 453. [CrossRef]
108. Corwin, D.L.; Rhoades, J.D. An Improved Technique for Determining Soil Electrical Conductivity-Depth Relations from Above-Ground Electromagnetic Measurements. *Soil Sci. Soc. Am. J.* **1982**, *46*, 517–520. [CrossRef]
109. Corwin, D.L.; Rhoades, J.D. Measurement of Inverted Electrical Conductivity Profiles Using Electromagnetic Induction. *Soil Sci. Soc. Am. J.* **1984**, *48*, 288–291. [CrossRef]
110. Cook, P.G.; Walker, G.R. Depth Profiles of Electrical Conductivity from Linear Combinations of Electromagnetic Induction Measurements. *Soil Sci. Soc. Am. J.* **1992**, *56*, 1015–1022. [CrossRef]
111. Johnston, M.A.; Savage, M.J.; Moolman, J.H.; Du Plessis, H.M. Evaluation of Calibration Methods for Interpreting Soil Salinity from Electromagnetic Induction Measurements. *Soil Sci. Soc. Am. J.* **1997**, *61*, 1627–1633. [CrossRef]
112. Coppola, A.; Smettem, K.; Ajeel, A.; Saeed, A.; Dragonetti, G.; Comegna, A.; Lamaddalena, N.; Vacca, A. Calibration of an Electromagnetic Induction Sensor with Time-Domain Reflectometry Data to Monitor Rootzone Electrical Conductivity under Saline Water Irrigation: The EMI Sensor for Salinity Management of the Rootzone. *Eur. J. Soil Sci.* **2016**, *67*, 737–748. [CrossRef]
113. Bennett, D.L.; George, R.J.; Whitfield, B. The Use of Ground EM Systems to Accurately Assess Salt Store and Help Define Land Management Options for Salinity Management. *Explor. Geophys.* **2000**, *31*, 249–254. [CrossRef]
114. Lesch, S. Statistical Models for the Prediction of Field-Scale and Spatial Salinity Patterns from Soil Conductivity Survey Data. In *Agricultural Salinity Assessment and Management*, 2nd ed.; ASCE: Reston, VA, USA, 2011; pp. 461–482. [CrossRef]
115. Corwin, D.L. Geospatial Measurements of Apparent Soil Electrical Conductivity for Characterizing Soil Spatial Variability. In *Soil-Water-Solute Process Characterization—An Integrated Approach*; Alvarez-Benedi, J., Munoz-Carpena, R., Eds.; CRC Press: Boca Raton, FL, USA, 1993; Volume 18, pp. 639–672.
116. Lu, L.; Li, S.; Wu, R.; Shen, D. Study on the Scale Effect of Spatial Variation in Soil Salinity Based on Geostatistics: A Case Study of Yingdaya River Irrigation Area. *Land* **2022**, *11*, 1697. [CrossRef]
117. Killick, M. An Analysis of the Relationship of Apparent Electrical Conductivity to Soil Moisture in Alluvial Recent Soils, Lower North Island, New Zealand. Master's Thesis, Massey University, Palmerston North, New Zealand, 2013. Available online: http://hdl.handle.net/10179/4902 (accessed on 21 July 2023).
118. Guo, Y.; Zhou, Y.; Zhou, L.; Liu, T.; Wang, L.; Cheng, Y.; He, J.; Zheng, G. Using Proximal Sensor Data for Soil Salinity Management and Mapping. *J. Integr. Agric.* **2019**, *18*, 340–349. [CrossRef]
119. Yao, R.; Yang, J. Quantitative Evaluation of Soil Salinity and Its Spatial Distribution Using Electromagnetic Induction Method. *Agric. Water Manag.* **2010**, *97*, 1961–1970. [CrossRef]
120. Jantaravikorn, Y.; Ongsomwang, S. Soil Salinity Prediction and Its Severity Mapping Using a Suitable Interpolation Method on Data Collected by Electromagnetic Induction Method. *Appl. Sci.* **2022**, *12*, 10550. [CrossRef]
121. Islam, M.M.; Saey, T.; Meerschman, E.; De Smedt, P.; Meeuws, F.; Van De Vijver, E.; Meirvenne, M. Delineating Water Management Zones in a Paddy Rice Field Using a Floating Soil Sensing System. *Agric. Water Manag.* **2011**, *102*, 8–12. [CrossRef]
122. Dakak, H.; Benmohammadi, A.; Soudi, B.; Douaik, A.; Badraoui, M.; Zouahri, A. Mapping the Risk of Soil Salinization Using Electromagnetic Induction and Non-Parametric Geostatistics. In *Developments in Soil Salinity Assessment and Reclamation*; Shahid, S.A., Abdelfattah, M.A., Taha, F.K., Eds.; Springer Netherlands: Dordrecht, The Netherlands, 2013; pp. 155–166. [CrossRef]

123. Xie, W.; Yang, J.; Yao, R.; Wang, X. Spatial and Temporal Variability of Soil Salinity in the Yangtze River Estuary Using Electromagnetic Induction. *Remote Sens.* **2021**, *13*, 1875. [CrossRef]
124. Gharsallah, M.E.; Aichi, H.; Stambouli, T.; Ben Rabah, Z.; Ben Hassine, H. Assessment and Mapping of Soil Salinity Using Electromagnetic Induction and Landsat 8 OLI Remote Sensing Data in an Irrigated Olive Orchard under Semi-Arid Conditions. *Soil Water Res.* **2022**, *17*, 15–28. [CrossRef]
125. Li, H.; Liu, X.; Hu, B.; Biswas, A.; Jiang, Q.; Liu, W.; Wang, N.; Peng, J. Field-Scale Characterization of Spatio-Temporal Variability of Soil Salinity in Three Dimensions. *Remote Sens.* **2020**, *12*, 4043. [CrossRef]
126. Farzamian, M.; Bouksila, F.; Paz, A.M.; Santos, F.M.; Zemni, N.; Slama, F.; Ben Slimane, A.; Selim, T.; Triantafilis, J. Landscape-Scale Mapping of Soil Salinity with Multi-Height Electromagnetic Induction and Quasi-3d Inversion in Saharan Oasis, Tunisia. *Agric. Water Manag.* **2023**, *284*, 108330. [CrossRef]
127. Paz, M.C.; Farzamian, M.; Paz, A.M.; Castanheira, N.L.; Gonçalves, M.C.; Monteiro Santos, F. Assessing Soil Salinity Dynamics Using Time-Lapse Electromagnetic Conductivity Imaging. *Soil* **2020**, *6*, 499–511. [CrossRef]
128. Farzamian, M.; Paz, M.C.; Paz, A.M.; Castanheira, N.L.; Gonçalves, M.C.; Monteiro Santos, F.A.; Triantafilis, J. Mapping Soil Salinity Using Electromagnetic Conductivity Imaging—A Comparison of Regional and Location-specific Calibrations. *Land Degrad. Dev.* **2019**, *30*, 1393–1406. [CrossRef]
129. Dakak, H.; Huang, J.; Zouahri, A.; Douaik, A.; Triantafilis, J. Mapping Soil Salinity in 3-Dimensions Using an EM38 and EM4Soil Inversion Modelling at the Reconnaissance Scale in Central Morocco. *Soil Use Manag.* **2017**, *33*, 553–567. [CrossRef]
130. Khongnawang, T.; Zare, E.; Srihabun, P.; Khunthong, I.; Triantafilis, J. Digital Soil Mapping of Soil Salinity Using EM38 and Quasi-3-d Modelling Software (EM4Soil). *Soil Use Manag.* **2021**, *38*, 277–291. [CrossRef]
131. Guo, Y.; Shi, Z.; Huang, J.; Wang, L.; Cheng, Y.; Zheng, G. Mapping Horizontal and Vertical Spatial Variability of Soil Salinity in Reclaimed Areas. In *Digital Soil Mapping Across Paradigms, Scales and Boundaries*; Zhang, G.-L., Brus, D., Liu, F., Song, X.-D., Lagacherie, P., Eds.; Springer Environmental Science and Engineering; Springer: Singapore, 2016; pp. 33–45. [CrossRef]
132. Dragonetti, G.; Farzamian, M.; Basile, A.; Monteiro Santos, F.; Coppola, A. In Situ Estimation of Soil Hydraulic and Hydrodispersive Properties by Inversion of Electromagnetic Induction Measurements and Soil Hydrological Modeling. *Hydrol. Earth Syst. Sci.* **2022**, *26*, 5119–5136. [CrossRef]
133. Dragonetti, G.; Comegna, A.; Ajeel, A.; Deidda, G.P.; Lamaddalena, N.; Rodriguez, G.; Vignoli, G.; Coppola, A. Calibrating Electromagnetic Induction Conductivities with Time-Domain Reflectometry Measurements. *Hydrol. Earth Syst. Sci.* **2018**, *22*, 1509–1523. [CrossRef]
134. Flores, J.G.; Rodríguez, M.R.; Jiménez, A.G.; Farzamian, M.; Herencia, J.F.; Galán, B.; Sacristan, P.C.; Vanderlinden, K. Monitoring Tridimensional Soil Salinity Patterns at the Field Scale Using Electromagnetic Induction Sensing and Inversion. *Salt-Affect. Soils* **2022**, *XV*, 48.
135. Borchers, B.; Uram, T.; Hendrickx, J.M.H. Tikhonov Regularization of Electrical Conductivity Depth Profiles in Field Soils. *Soil Sci. Soc. Am. J.* **1997**, *61*, 1004–1009. [CrossRef]
136. Hendrickx, J.M.H.; Borchers, B.; Corwin, D.L.; Lesch, S.M.; Hilgendorf, A.C.; Schlue, J. Inversion of Soil Conductivity Profiles from Electromagnetic Induction Measurements: Theory and Experimental Verification. *Soil Sci. Soc. Am. J.* **2002**, *66*, 673–685. [CrossRef]
137. Gebbers, R.; Lück, E.; Heil, K. Depth Sounding with the EM38-Detection of Soil Layering by Inversion of Apparent Electrical Conductivity Measurements. *Precis. Agric.* **2007**, *7*, 95–102. [CrossRef]
138. Moghadas, D.; Jadoon, K.Z.; McCabe, M.F. Spatiotemporal Monitoring of Soil Moisture from EMI Data Using DCT-Based Bayesian Inference and Neural Network. *Appl. Geophys.* **2019**, *169*, 226–238. [CrossRef]
139. Triantafilis, J.; Santos, F.A.M.; Triantafilis, J.; Santos, F.A.M. Resolving the Spatial Distribution of the True Electrical Conductivity with Depth Using EM38 and EM31 Signal Data and a Laterally Constrained Inversion Model. *Soil Res.* **2010**, *48*, 434–446. [CrossRef]
140. Triantafilis, J.; Santos, F.A.M. 2-Dimensional Soil and Vadose-Zone Representation Using an EM38 and EM34 and a Laterally Constrained Inversion Model. *Soil Res.* **2009**, *47*, 809. [CrossRef]
141. Moghadas, D.; Taghizadeh-Mehrjardi, R.; Triantafilis, J. Probabilistic Inversion of EM38 Data for 3D Soil Mapping in Central Iran. *Geoderma Reg.* **2016**, *7*, 230–238. [CrossRef]
142. Paz, M.C.; Farzamian, M.; Santos, F.M.; Gonçalves, M.C.; Paz, A.M.; Castanheira, N.L.; Triantafilis, J. Potential to Map Soil Salinity Using Inversion Modelling of EM38 Sensor Data. *First Break* **2019**, *37*, 35–39. [CrossRef]
143. Paz, A.M.; Castanheira, N.; Farzamian, M.; Paz, M.C.; Gonçalves, M.C.; Monteiro Santos, F.A.; Triantafilis, J. Prediction of Soil Salinity and Sodicity Using Electromagnetic Conductivity Imaging. *Geoderma* **2020**, *361*, 114086. [CrossRef]
144. Jadoon, K.Z.; Moghadas, D.; Jadoon, A.; Missimer, T.M.; Al-Mashharawi, S.K.; McCabe, M.F. Estimation of Soil Salinity in a Drip Irrigation System by Using Joint Inversion of Multicoil Electromagnetic Induction Measurements. *Water Resour. Res.* **2015**, *51*, 3490–3504. [CrossRef]
145. Farzamian, M.; Monteiro Santos, F.A.; Khalil, M.A. Application of EM38 and ERT Methods in Estimation of Saturated Hydraulic Conductivity in Unsaturated Soil. *Appl. Geophys.* **2015**, *112*, 175–189. [CrossRef]
146. Martini, E.; Werban, U.; Zacharias, S.; Pohle, M.; Dietrich, P.; Wollschläger, U. Repeated Electromagnetic Induction Measurements for Mapping Soil Moisture at the Field Scale: Validation with Data from a Wireless Soil Moisture Monitoring Network. *Hydrol. Earth Syst. Sci.* **2017**, *21*, 495–513. [CrossRef]

147. Farzamian, M.; Autovino, D.; Basile, A.; De Mascellis, R.; Dragonetti, G.; Monteiro Santos, F.; Binley, A.; Coppola, A. Assessing the Dynamics of Soil Salinity with Time-Lapse Inversion of Electromagnetic Data Guided by Hydrological Modelling. *Hydrol. Earth Syst. Sci.* **2021**, *25*, 1509–1527. [CrossRef]
148. Von Hebel, C.; Rudolph, S.; Mester, A.; Huisman, J.A.; Kumbhar, P.; Vereecken, H.; Van Der Kruk, J. Three-Dimensional Imaging of Subsurface Structural Patterns Using Quantitative Large-Scale Multiconfiguration Electromagnetic Induction Data. *Water Resour. Res.* **2014**, *50*, 2732–2748. [CrossRef]
149. Taghizadeh-Mehrjardi, R.; Minasny, B.; Sarmadian, F.; Malone, B.P. Digital Mapping of Soil Salinity in Ardakan Region, Central Iran. *Geoderma* **2014**, *213*, 15–28. [CrossRef]
150. Wang, F.; Yang, S.; Wei, Y.; Shi, Q.; Ding, J. Characterizing Soil Salinity at Multiple Depth Using Electromagnetic Induction and Remote Sensing Data with Random Forests: A Case Study in Tarim River Basin of Southern Xinjiang, China. *Sci. Total Environ.* **2021**, *754*, 142030. [CrossRef] [PubMed]
151. McBratney, A.B.; Mendonça Santos, M.L.; Minasny, B. On Digital Soil Mapping. *Geoderma* **2003**, *117*, 3–52. [CrossRef]
152. Rentschler, T. Explainable Machine Learning in Soil Mapping: Peeking into the Black Box. Ph.D. Thesis, Universität Tübingen, Tübingen, Germany, 2021. [CrossRef]
153. Taghizadeh-Mehrjardi, R.; Ayoubi, S.; Namazi, Z.; Malone, B.P.; Zolfaghari, A.A.; Sadrabadi, F.R. Prediction of Soil Surface Salinity in Arid Region of Central Iran Using Auxiliary Variables and Genetic Programming. *Arid. Land Res. Manag.* **2016**, *30*, 49–64. [CrossRef]
154. Sahbeni, G.; Ngabire, M.; Musyimi, P.K.; Székely, B. Challenges and Opportunities in Remote Sensing for Soil Salinization Mapping and Monitoring: A Review. *Remote Sens.* **2023**, *15*, 2540. [CrossRef]
155. Farifteh, J.; Farshad, A.; George, R.J. Assessing Salt-Affected Soils Using Remote Sensing, Solute Modelling, and Geophysics. *Geoderma* **2006**, *130*, 191–206. [CrossRef]
156. Aldabaa, A.A.A.; Weindorf, D.C.; Chakraborty, S.; Sharma, A.; Li, B. Combination of Proximal and Remote Sensing Methods for Rapid Soil Salinity Quantification. *Geoderma* **2015**, *239–240*, 34–46. [CrossRef]
157. Casterad, M.A.; Herrero, J.; Betrán, J.A.; Ritchie, G. Sensor-Based Assessment of Soil Salinity during the First Years of Transition from Flood to Sprinkler Irrigation. *Sensors* **2018**, *18*, 616. [CrossRef] [PubMed]
158. Allbed, A.; Kumar, L. Soil Salinity Mapping and Monitoring in Arid and Semi-Arid Regions Using Remote Sensing Technology: A Review. *Adv. Remote Sens.* **2013**, *2*, 373–385. [CrossRef]
159. Metternicht, G.I.; Zinck, J.A. Remote Sensing of Soil Salinity: Potentials and Constraints. *Remote Sens. Environ.* **2003**, *85*, 1–20. [CrossRef]
160. Scudiero, E.; Skaggs, T.H.; Corwin, D.L. Comparative Regional-Scale Soil Salinity Assessment with near-Ground Apparent Electrical Conductivity and Remote Sensing Canopy Reflectance. *Ecol. Indic.* **2016**, *70*, 276–284. [CrossRef]
161. Rao, B.R.M.; Sharma, R.C.; Ravi Sankar, T.; Das, S.N.; Dwivedi, R.S.; Thammappa, S.S.; Venkataratnam, L. Spectral Behaviour of Salt-Affected Soils. *Int. J. Remote Sens.* **1995**, *16*, 2125–2136. [CrossRef]
162. Wu, W.; Mhaimeed, A.S.; Al-Shafie, W.M.; Ziadat, F.; Dhehibi, B.; Nangia, V.; De Pauw, E. Mapping Soil Salinity Changes Using Remote Sensing in Central Iraq. *Geoderma Reg.* **2014**, *2–3*, 21–31. [CrossRef]
163. Sultanov, M.; Ibrakhimov, M.; Akramkhanov, A.; Bauer, C.; Conrad, C. Modelling End-of-Season Soil Salinity in Irrigated Agriculture Through Multi-Temporal Optical Remote Sensing, Environmental Parameters, and In Situ Information. *PFG–J. Photogramm. Remote Sens. Geoinf. Sci.* **2018**, *86*, 221–233. [CrossRef]

Disclaimer/Publisher's Note: The statements, opinions and data contained in all publications are solely those of the individual author(s) and contributor(s) and not of MDPI and/or the editor(s). MDPI and/or the editor(s) disclaim responsibility for any injury to people or property resulting from any ideas, methods, instructions or products referred to in the content.